CHALMERS

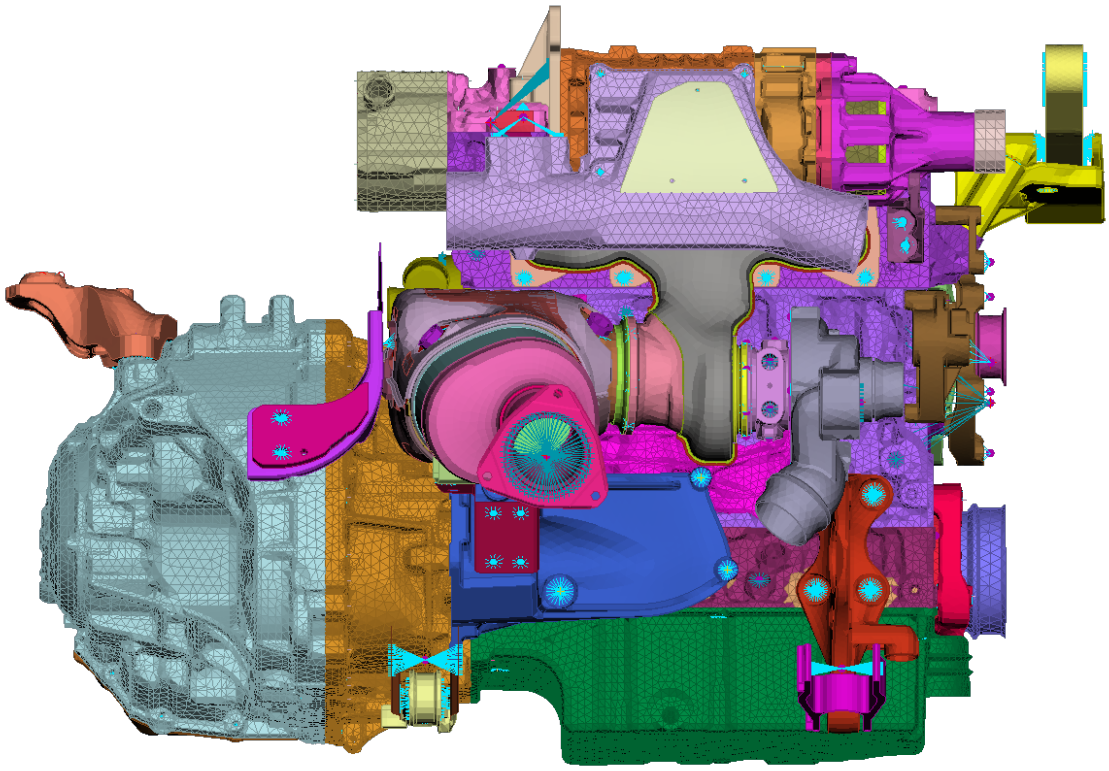

Countermeasures for Impulsive Noise Character in Internal Combustion Engines

Master's thesis in Applied Mechanics

ALEXANDER OLSSON

Department of Mechanics and Maritime Sciences
CHALMERS UNIVERSITY OF TECHNOLOGY
Göteborg, Sweden 2019

MASTER'S THESIS IN APPLIED MECHANICS

Countermeasures for Impulsive Noise Character in Internal Combustion Engines

ALEXANDER OLSSON

Department of Mechanics and Maritime Sciences

Division of Dynamics

CHALMERS UNIVERSITY OF TECHNOLOGY

Göteborg, Sweden 2019

Countermeasures for Impulsive Noise Character in Internal Combustion Engines
ALEXANDER OLSSON

© ALEXANDER OLSSON, 2019

Master's thesis 2018:94
Department of Mechanics and Maritime Sciences
Division of Dynamics
Chalmers University of Technology
SE-412 96 Göteborg
Sweden
Telephone: +46 (0)31-772 1000

Cover:
The cover shows the discretized model of the entire engine from a front view. It can be found in Figure 2.1(a), where also the main parts of the engine is labelled on top of the figure.

Countermeasures for Impulsive Noise Character in Internal Combustion Engines
Master's thesis in Applied Mechanics
ALEXANDER OLSSON
Department of Mechanics and Maritime Sciences
Division of Dynamics
Chalmers University of Technology

Abstract

The demand for efficient vehicle propulsion has led to downsizing of the internal combustion engines. Combined with a request for increased power output, these engines experience high peak pressures and strong pressure gradients. The downsizing strategy has been found to induce noise that has an impulsive character. This project investigates ways to counteract the transfer of this noise into the vehicle cabin. The assessment of the impulsive noise character is based on the peak to average power ratio, spectrograms and subjective listening of the vibration time history signal in the mounting points between the engine and the car. The evaluation has also been aided by an overall sound pressure level estimate. The analysis is carried out using an existing discretized model of a spark ignited four cylinder four stroke internal combustion engine. The influence of material density, material stiffness, combustion strategy and bearing clearance on the generation of impulsive noise character is investigated in a parameter study. Moreover, the possible mitigation of the noise character is investigated in a design study, where the attachments in the engine structure of one of the mounting points between the engine and the car are changed, while maintaining the position of the mounting point to the car.

It is concluded that an increased crank shaft stiffness, a prolonged combustion duration and a redesigned suspension console are the three most efficient countermeasures to diminish the noise character.

Keywords: Impulsive noise character, Impulsiveness, Impulsive noise, Car noise, Internal combustion engine

Preface

This master's thesis project is carried out at Volvo Car Corporation's Research and Development organisation, at the Engine CAE Solids Team within Propulsion Power Systems. It corresponds to 30 credit points and has been carried out over a period of 20 weeks. The purpose is to be both educational for the writer and the reader, as well as provide a beneficial contribution to Volvo Cars in their pursuit of unprecedented quality.

The aim of the project is to give relevant insight into what can be done to reduce the impulsive noise character heard from the internal combustion engine in the car cabin. The impulsive noise character is regarded as annoying and in principal a non-desired sound characteristic for a car. Although no definitive limit between good and bad engine sounds exists, due to its highly subjective nature, the impulsive noise character is mainly perceived as annoying regardless of how loud or predominant it is. The impulsive noise character would not be considered problematic if only occurring when demanding high loads, however the presence at moderate operating scenarios is undesirable.

The reduction of the impulsive noise character is of great importance for future engine generations. In the pursuit of a minimised environmental impact, the engines are getting smaller and smaller and at the same time operated in more and more demanding ways. The combination is potentially catastrophic from a noise generation perspective, possibly yielding unacceptable noise levels and characteristics. By enabling the car industry to better control the sound signature of their engines they may not only develop more desirable cars, but at the same time enable further environmental optimisation. The ambition for this thesis is to aid both of those possibilities.

The political landscape for vehicle propulsion may be uncertain, but it is safe to say that the internal combustion engine will play a big role for a foreseeable future in the car industry. With the possibility to run on many types of fuels, some renewable and thus effectively more or less emission free and CO_2 neutral, it may remain as the dominating propulsion system for many years to come.

Acknowledgements

During the thesis I have had the privilege to work with some awe-inspiring people, which I would like to commemorate. I would like to dedicate my most sincere and wholehearted gratitude to Johan Cederlund for your endless and unfailing support. For your mentoring I am hugely grateful. A special thanks to Peter Torstensson for your invaluable backing and assistance throughout the project. Henrik Hedberg and Andreas Berntsson also deserves a special thanks for providing me with input and aid. Thank you Håkan Johansson for taking time to examine this thesis and endure my numerous emails. I would like to credit all colleagues at Volvo Cars for your warm welcome and allowing me to be part of your daily work life. You made my stay a tremendously pleasant one. Finally I am profoundly grateful to all my friends and family for your encouragement and company and most of all my parents, whom I am indebted to for your unconditional love and faith.

Alexander Olsson

Gothenburgh
January 2019

Nomenclature

Abbreviations

DOF	Degree Of Freedom
EATS	Exhaust After Treatment System
EEM	Elementary Effects Method
FFT	Fast Fourier Transform
GSA	Global Sensitivity Analysis
LHM	Left Hand Mount
LLTB	Left Lower Tie Bar
LSA	Local Sensitivity Analysis
NVH	Noise Vibration and Harshness
OFAT	One Factor At a Time
PAPR	Peak To Average Power Ratio
RHM	Right Hand Mount
RLTB	Right Lower Tie Bar
RMS	Root Mean Square
RUTB	Right Upper Tie Bar
SA	Sensitivity Analysis
SEM	Standard Error of the Mean
SD	Standard Deviation
STFT	Short Time Fourier Transform
TDC	Top Dead Centre

Contents

List of Figures

List of Tables

1 Introduction

The following chapter covers a background to the problem, as well as a detailed project clarification and description.

1.1 Background

With increasing demand for higher efficiency, lower emission and reduced fuel consumption for internal combustion engines, the automotive industry tend to downsize their internal combustion engines in order to minimise friction and increase specific power. Combined with an increased power demand, these modern downsized combustion engines experience high peak pressures and strong pressure gradients.

This strategy has been found to induce noise that has an impulsive character. This makes the engine sound rough and growling in operating scenarios with moderate engine speeds and loads. The presence at high loads would not be considered problematic, however at moderate operating scenarios it is desirable to diminish the impulsive noise character. Thus the investigation of noise, vibration and harshness (NVH) is more important than ever in order to guarantee an engine that performs well in all aspects.

At Volvo Cars there is an interest in evaluating countermeasures to suppress the impulsive noise character in both current engines as well as in engines under development. In addition, Volvo Cars likes to further develop available computational tools in order to improve their understanding of the impulsive noise character and to determine mitigation actions already in the design phase.

1.2 Aim

This project will use computer aided engineering to investigate the influence of selected parameters on the generation of the impulsive noise character in internal combustion engines. The aim is to propose efficient mitigation actions for engines currently in production. Furthermore engines in development will be investigated as well, meaning that design changes can be considered. The available computational tools and procedures will be further developed. The proposition of efficient countermeasures to the impulsive noise character is to be considered the ultimate goal of the project.

1.3 Limitations

The following limitations will be made, mainly due to time restrictions:

- Only one model of a spark ignited internal combustion engine currently in production will be investigated and modified.
- Only structure borne noise will be investigated (i.e. no airborne noise will be considered).
- Available models and simulation methods will be used.

1.4 Work plan

Based on the aim of the project, the following goals have been determined:

- To perform a literature study to review the state of knowledge of the current problem.
- To understand and describe the impulsive noise character of the internal combustion engine and the noise generation in the vehicle cabin.

- To identify the most important parameters for the impulsive noise character.
- To understand and describe the existing discretized engine model and solution process/method currently in use at Volvo Cars. If needed, tune the process to better suit the investigation.
- To perform a parameter study to investigate the influence of important parameters for the generation of impulsive noise. Based on the results the most efficient countermeasures are suggested.
- To perform a model design change study to investigate the influence of design changes to the problem. Based on the results the most efficient countermeasures are suggested.
- To discuss the current computational tools used to evaluate the impulsive noise character.
- To document and present all above in a clear way.

1.5 Ethics, environmental and society perspectives

The project is not believed to contain any controversial aspects. The reduction of impulsive noise generation in internal combustion engines can be considered a key factor to enable more efficient combustion vehicle propulsion, and thus this project might have an indirect positive environmental impact. The work relies on computational simulations and as experimental tests are absent the use of fossil fuel, and thereby caused emissions, will not be a concern as part of the current project. Before incorporating design changes to minimise the impulsive noise character it is needed to be investigated if those are believed to have any impact, positive or negative, on the engine fuel consumption.

From an environmental perspective the investigation of internal combustion engines typically focuses on fuel consumption and effective combustion. However, the reduction of impulsive noise generated from the internal combustion engine have a direct positive effect on noise pollution, and may also reduce pass-by-noise. In dense cities noise pollution could be considered a concern of public health, and the reduction of the same crucial for well being.

2 Analysis of impulsive noise character

The ability to propose countermeasures to the impulsive noise character requires knowledge of root causes, what is actually meant by *impulsiveness* and why it may be a disconcert.

In this chapter key aspects of the phenomenon are presented, together with a literature review. Moreover, the applied numerical model is described.

2.1 Essential concepts

Essential concepts related to the understanding and evaluation of the impulsive noise character are presented below.

2.1.1 Loudness

The human perception of sound is complex. Physical metrics may fail to adequately represent perceived sound. Frequency content, bandwidth and time aspects are all relevant to understand the human perception of sound. The introduction of the subjective metric *loudness* is required to quantify how loud a certain sound pressure level is perceived. Loudness is measured in sone [1]. In this project the impulsive noise character of the internal combustion engine is investigated. For this type of sound, consisting of short pulses, the perceived loudness is reduced if the duration of the pulse is shorter than approximately 200 ms. A pure tone with duration 10 ms would have to be increased by approximately 10 dB to be experienced equally loud as a continuous tone. Furthermore, sound that includes a broadband frequency content is perceived louder as compared with a tonal sound at a corresponding sound pressure level. In addition, the human hearing is not equally sensitive at different frequencies meaning that weighting has to be considered to correctly represent how loud different frequencies are perceived [1].

2.1.2 Impulsiveness

The term impulsiveness is used to describe the character of the studied sound phenomenon. Within the car industry several terms are being used to categorise sound. For the internal combustion engine, and in this project, impulsiveness and roughness are two important sound characteristics. There seem to exist no definition to exactly what these are, and the terms are used differently. In this project impulsiveness is defined as *short sound pulses with broadband frequency content where consecutive pulses can be separated by the human ear, meaning that the modulation of the sound is distinguishable.* The related term roughness refers to the same type of sound pulses, however modulated at higher frequencies. The term impulsiveness is in this project used to categorise this type of sound with a modulation frequency of up to approximately 30 Hz, after which the human ear can no longer distinguish between the individual events.

2.1.3 Engine orders

The internal combustion engine is a reciprocating machine, and any imbalance will induce vibrations. These vibrations are categorised by how they relate to the engine speed, referenced by the crank shaft. Excitation that occurs once per revolution is referred to as the first order vibration of the engine. Accordingly, the second order vibration of the engine corresponds to excitation that occurs twice per revolution, and so on. Excitation that occurs every second revolution is referred to as the engine half order. The cylinder ignition events are the main excitation mechanism for an internal combustion engine. For a four cylinder four stroke engine that corresponds to the second engine order, since ignition events occur twice per revolution. The mass loads from e.g. the pistons do also correspond to the second order for a four stroke four cylinder engine. The presence and combination of the infinitely many engine orders is one important part in the understanding of the characteristic sound of a specific engine.

For the impulsive noise character sought to be diminished in this project, the ignition in cylinder number 1 is believed to be the root cause. Since investigating a four cylinder four stroke engine cylinder number 1 ignites every second revolution, and the engine half order is thus of extra interest in this project.

In the studied engine the cylinder ignition scheme is, numbered from the right hand side, 1-3-4-2. The ignition events occur with 180 degrees crank shaft angle separation. The first cylinder piston is at top dead centre (TDC) at 0 degrees, and the ignition event occurs at closely related crank shaft angles.

See Figure 2.1 for an understanding of the location of the different cylinders.

2.2 Problem description

At moderate engine speeds and loads an impulsive noise character can be perceived in the vehicle cabin. The noise includes a broad range of frequency components and is modulated at frequencies of up to approximately 30 Hz.

The modulation frequency corresponds to the four cylinder four stroke engine half order (once per two revolutions), and the cylinder ignition impulse at the right hand most cylinder of the engine has been identified as the main noise excitation mechanism. The modulation frequency stems from the rotational speed of the engine. Particularly the range between 1500 rpm to 3000 rpm is considered as problematic. Note that at modulation frequencies that exceed 30 Hz the impulsive noise character becomes less distinct and the noise is rather perceived as continuous. According to Section 2.1.2 this is the inflection point between the two terms impulsiveness and roughness. The half order of the engine is modulating with a frequency of 30 Hz when rotating at 3600 rpm, meaning that noise generated at engine speeds exceeding this will not be perceived as impulsive, but rather rough and is thus not accounted for in this project.

The root cause of the impulsive noise character is the excitation of the engine structure from the cylinder ignition events. These excitations trigger natural modes in the engine structure that propagates via the engine mounts into the cabin. Due to its close coupling to the right hand most cylinder, the right hand engine mount is particularly important to analyse, see Figure 2.1. It is believed that the mass-stiffness ratio between the cylinder head and engine mount, and base structure and engine mount, respectively, are causes to the problem.

The subjective perception of the impulsiveness inherited in the generated noise is related to the driving scenario at which it occurs. If at full throttle and high speeds, the noise could actually be perceived as powerful and convincing, enhancing the performance experience of the car and engine. However, the occurrence at other scenarios is considered problematic and unwanted.

2.3 Literature review

In [2] several interesting aspects related to this thesis are discussed. The authors have studied how the crank shaft stiffness and main bearing tolerances affect the NVH performance of a four cylinder petrol powered internal combustion engine. Using mainly velocity and acceleration as evaluation metrics it was concluded that the stiffness of the crankshaft was the most important parameter to control the NVH performance of the engine, followed by the main bearing tolerance. Indications of when to expect impulsive noise phenomena from the engine are stated to include mount bracket vibrations and large contents of half orders in the analysed vibration signals. It is concluded that noise in the range 200 Hz to 800 Hz is most important with respect to engine roughness.

As concluded by [3] the perceived noise quality rather than the actual noise sound pressure level is of importance to evaluate the acoustic performance inside a vehicle cabin. In the article a model to predict presence of internal combustion engine roughness is presented. It is stated that the engine roughness occurs in a frequency range where structure borne noise is dominating, according to the article 100 Hz to 1000 Hz, thus motivating and allowing for the air borne noise to be neglected in the comparative simulation analysis. At Volvo Cars the same conclusion has been made based on measurements. Similarly this project will not account for air borne noise radiated from the surfaces of the engine.

A related discussion about psychoacoustics and the fact that perceived sound quality not necessarily corresponds to reduced sound pressure levels is made in [4]. In the article it is stated that: *"It is assumed that the perception of impulsiveness is mainly caused by relative variation of loudness over time"*. The article presents sound mapping techniques and implements several metrics, such as loudness in varying forms, roughness, sharpness and impulsiveness.

The use of several noise evaluation metrics is discussed in [5]. This work does not only discuss sound pressure level in relation to perceived sound quality, but also the development of a new objective metric to better account for the subjective perception of impulsive noise from internal combustion engines. The model for simulation of impulsive noise described in [6, 7, 5] is implemented and evaluated. The frequency range of 500 Hz to 12 500 Hz is considered. The article motivates why traditional sound quality metrics such as time-varying loudness are insufficient and expresses the need for new assessment criterions.

In [8] a more generalised perspective to the analysis of engine vibrations is given, that does not take direct consideration of psychoacoustic events. The general vibration problem of modern internal combustion engine is pinpointed as: *"The challenge is to keep vibrations on an acceptable level while output power increases and structures become lighter"*. The article gives insight in the standard procedure to analyse vibration as the root mean square (RMS) of the velocity. A RMS velocity threshold of $28\,\mathrm{mm\,s^{-1}}$ at the engine block is proposed. Information about the importance of natural modes and also the relation between local and global vibration is stated. Resonances are considered possibly acceptable if the direction of excitation does not correspond to one that effectively excites the natural mode shape.

Generally it can be said that the definition of impulsive noises is not stringent. It is possibly so that what some author may describe as roughness is what some other author would describe as impulsiveness. The importance of the choice of sound quality metrics, and possibly the development of a new type of assessment criterion for disturbances due to impulsiveness, is relevant for this thesis. The fact that the impulsive noise is a so called psychoacoustic phenomenon makes it hard to quantify and thus to evaluate using traditional metrics.

2.4 Engine modelling

The modelled engine consists of the following main parts:

- AC compressor
- Alternator
- Balancer shafts (*not visible*)
- Bed plate
- Block
- Camshafts
- Connecting rods (*not visible*)
- Cylinder head
- Exhaust after treatment system (EATS)
- Fuel pump (*not visible*)
- Gear box (without gears)
- Oil pump (*not visible*)
- Oil sump
- Starter motor
- Supercharger
- Turbocharger
- Vacuum pump
- Water pump

Hereafter, all these will be referred to as the *entire engine*. The entire engine without the crank shaft, the balancer shafts and the connecting rods, i.e. the stationary parts of the engine, will be referred to as the *power unit*.

The five connection points between the engine and the car, where noise may be structure borne into the cabin, are of particular importance in this project. These five are:

- Left hand mount (LHM)
- Left lower tie bar (LLTB)
- Right hand mount (RHM)
- Right lower tie bar (RLTB)
- Right upper tie bar (RUTB)

The five connection points consist of two suspension points (LHM and RHM) and three torque absorbing bars (LLTB, RLTB and RUTB), all connected to the car with dampening orthotropic rubber bushings. They are shown and labelled in Figure 2.1.

Figure 2.1(a) and Figure 2.1(b) show the front side and the back side of the engine, respectively. The main engine parts listed above are labelled on top or near the part itself. Note that some components are not visible.

2.4.1 Discretization

An existing model of the complete engine, set up in pre-processor ANSA [9], is used. The model uses both solid elements and shell elements, and mixed mesh types. The discretized model consists of a total of 14 254 398 (power unit) + 3 666 666 (crank shaft) + approximately 160 000 (two balancer shafts) + approximately 240 (four connecting rods) degrees of freedom (DOFs). In order to make the computational cost reasonable the model is condensed, by performing a so called local-global analysis in MSC NASTRAN [10]. Here so called superelements are created to represent flexible bodies. If desired, a modal analysis is performed in MSC NASTRAN yielding mass- and stiffness matrices and natural mode shapes and frequencies. These can be viewed and analysed in post-processor META [11].

The condensed model has reduced the initial DOFs to a total of 5 667 static DOFs and 504 modal DOFs for the power unit, 420 static DOFs for the crank shaft, 12 static DOFs for each of the four connecting rods and 60 static DOFs for each of the two balancer shafts. The complex structure of the power unit requires the modal DOFs to capture the natural mode shapes correctly. The shafts are lumped mass models for which the modal shapes will be accurately described, without the need for generalised DOFs.

2.4.2 Multi body dynamics

The data from the condensed models are used as input in the multibody dynamics software AVL EXCITE [12]. Interactions between stationary and rotating bodies, bearing properties, cylinder pressure data et cetera are stated. AVL EXCITE simulates the dynamic behaviour of the mechanical system accounting for structural flexibility and kinematic couplings such as e.g. roller bearings, plain bearings and cylindrical gear joints. The schematic set up in AVL EXCITE is found in Figure 2.2. The most noticeable changes from the real engine is the lack of cylindrical gears within the gearbox and that the brake torque is applied directly at the torque converter instead of at the differential(s)/wheel axle(s). The constant brake torque is calculated as a nominal torque, and then corrected to account for losses such as friction to maintain a steady engine speed in the simulations. The simulation is set to have an initial speed, and then the cylinder pressure data virtually runs the engine. A maximum mean engine speed increase or decrease during the simulation of 1 % and a maximum offset from expected mean engine speed to actually simulated mean engine speed of 10 rpm during two engine cycles is typically the case. The power unit structure is set to have no rigid body motion, meaning that only elastic natural modes are present in the results. The model is believed to accurately capture modal behaviour of up to approximately 500 Hz. For higher frequency modal behaviour the uncertainty of the results grows with increased frequency.

There is no surrounding car structure to mount the engine to, hence the five connection points, RHM, LHM, RUTB, RLTB and LLTB, are connected to a completely rigid structure (ground). The connection points are mounted using rubber bushings, with stiffness and damping properties that vary between the different connection points and spatial directions, however without accounting for frequency dependent properties.

The simulation is set to run for six complete cycles, and the results are recorded for the two last cycles. In the presented data and plots in the result sections the label of the axis for the crank angle has been shifted to 0 degrees to simplify the understanding. Engine speeds in steps of 250 rpm have been evaluated.

2.5 Evaluation of impulsiveness

The simulation results have been evaluated with respect to the impulsive noise character using three different quantities. The three tools yield information that together is believed to capture the psychoacoustic impulsive

noise character. The evaluation tools all utilise the time history data of quantities such as acceleration or velocity in the five mounting points between the engine and the car. Below follows a description of the three.

2.5.1 Peak to average power ratio

The evaluation of impulsiveness is predominately based on the peak to average power ratio (PAPR) of the vibration signal in the RHM and in the RLTB. The PAPR is defined as the squared ratio between peak values and the root mean square (RMS) value, as:

$$a_{\text{PAPR}} = \left(\frac{a_{\text{peak}}}{a_{\text{RMS}}} \right)^2 \tag{2.1}$$

By using the PAPR, instead of e.g. the peak values, two beneficial advantages arise; (1) a more fluctuating signal, and thus presumably more impulsive, would yield higher PAPR values and (2) since comparing the peak values to the RMS value of the signal the masking of the impulsiveness is taken into account meaning that some basic human sound perception aspects are taken into account. The historic usage and proven validity of this evaluation metric to determine impulsiveness at Volvo Cars is a third reason for it to be applied in the current work.

For this project the RMS value is calculated over two cycles (four full engine revolutions), meaning that the RMS is constant for each of the evaluated cases. In Figure 2.3 an example of a PAPR evaluation is presented, combined with the original time history signal and the RMS value. Note how the PAPR is always positive.

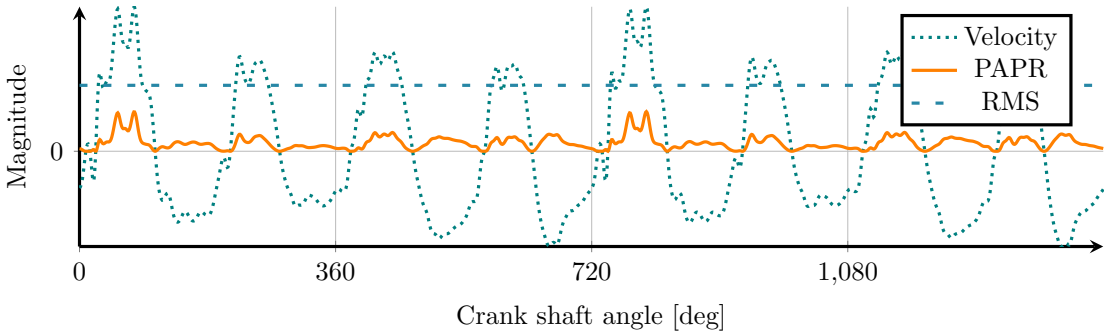

Figure 2.3: Time history data and the corresponding RMS and PAPR values.

2.5.2 Spectrogram

To analyse the frequency contents and its variation in time, and how it relates to the crank shaft rotational position, a spectrogram is helpful. A spectrogram consists of two axes, one for time and one for frequency, presenting how the sound varies in time as a surface for visual assessment.

Engine rotational speeds between 1500 rpm to 3600 rpm typically corresponds to a combustion duration of approximately 3.1 ms to 1.3 ms, respectively. Since the combustion events are important in order to understand the impulsiveness of the engine, it is desirable to capture the frequency content and its variation in related time scales. A short time Fourier transform (STFT) [13] is performed on the time history data, transforming it into the frequency domain. A fast Fourier transform (FFT) is performed on the already transformed signal to relate the cyclic occurrence of the frequency contents with the engine orders, enabling identification of possible noise sources. The result provides understanding of the frequency content and how it varies during the engine revolution cycles.

A traditional FFT would not be able to calculate spectra with the equivalent time resolution as in the time history data. The solution is to use a windowing function to transform short time intervals of the signal. This does however introduce a problem of low resolution in the frequency domain. A wider window would yield a lower resolution in time but higher in frequency, and vice versa. To accommodate for this the windowing is set

to overlap, enabling a pseudo-increased resolution in frequency domain while keeping the time resolution high enough to capture combustion related events. To minimise the unwanted overlapping effects a Hann window is used to capture mainly the centre of the window. The result is a spectrogram with enough resolution in both time- and frequency domains to capture the cylinder combustion events. Note that the resolution above is not related to the signal sampling resolution, which, however, also has to be high enough to yield relevant results.

2.5.3 Subjective listening

The vertical time history data from the RHM is translated into a synthesised sound file. The velocity time history data for 1500 rpm is used. Two revolutions at this engine speed take 0.08 s. To extend the sound file to a more accessible time scale the signal is sequentially added to itself several times. The signal is low pass filtered and normalised to its RMS-value to make comparisons between different cases viable. These sound files are not what the engine would sound like in the cabin, however is believed to accurately represent what type of sound signature to expect.

The synthesised sound files are evaluated using informal listening as a complement to the other two evaluation methods. The listening may provide extra certainty to conclusions, however may not be used as a stand alone evaluation method.

Note that, due to the RMS normalisation, the subjective listening may only give information about the character of the evaluated case, not assess the overall acoustic performance.

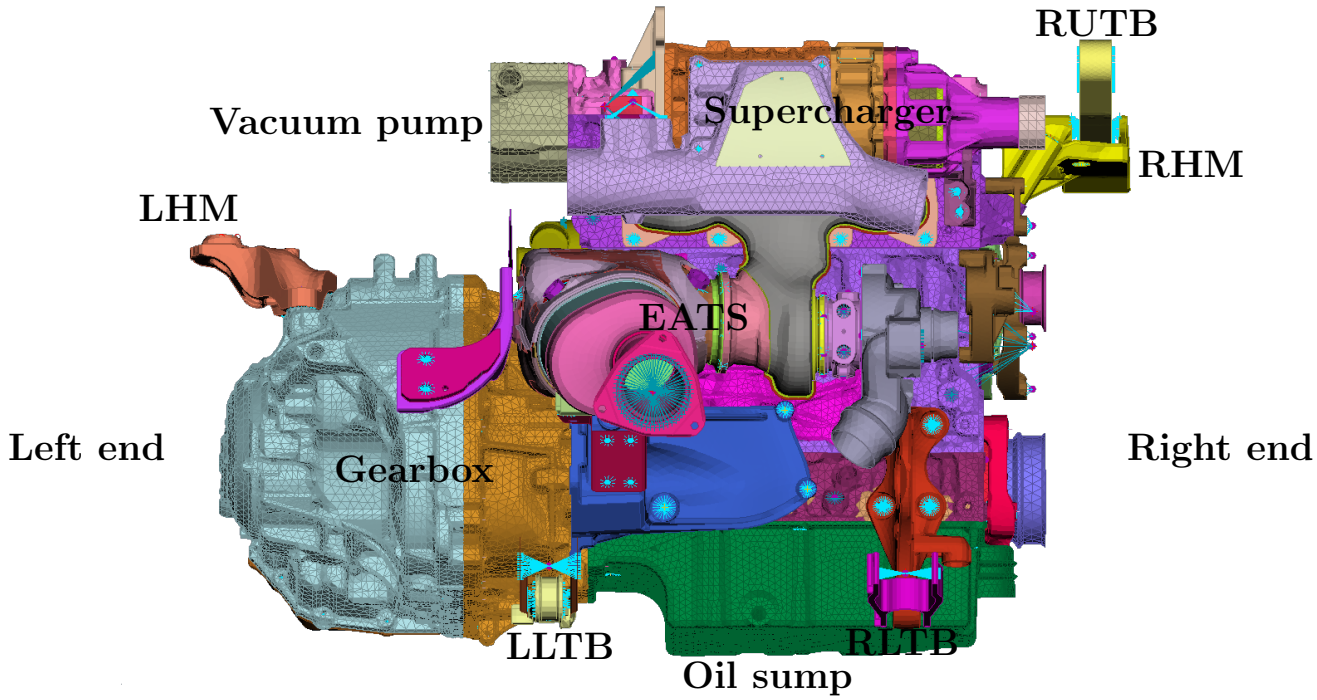

(a) The front side of the engine labelled with main parts.

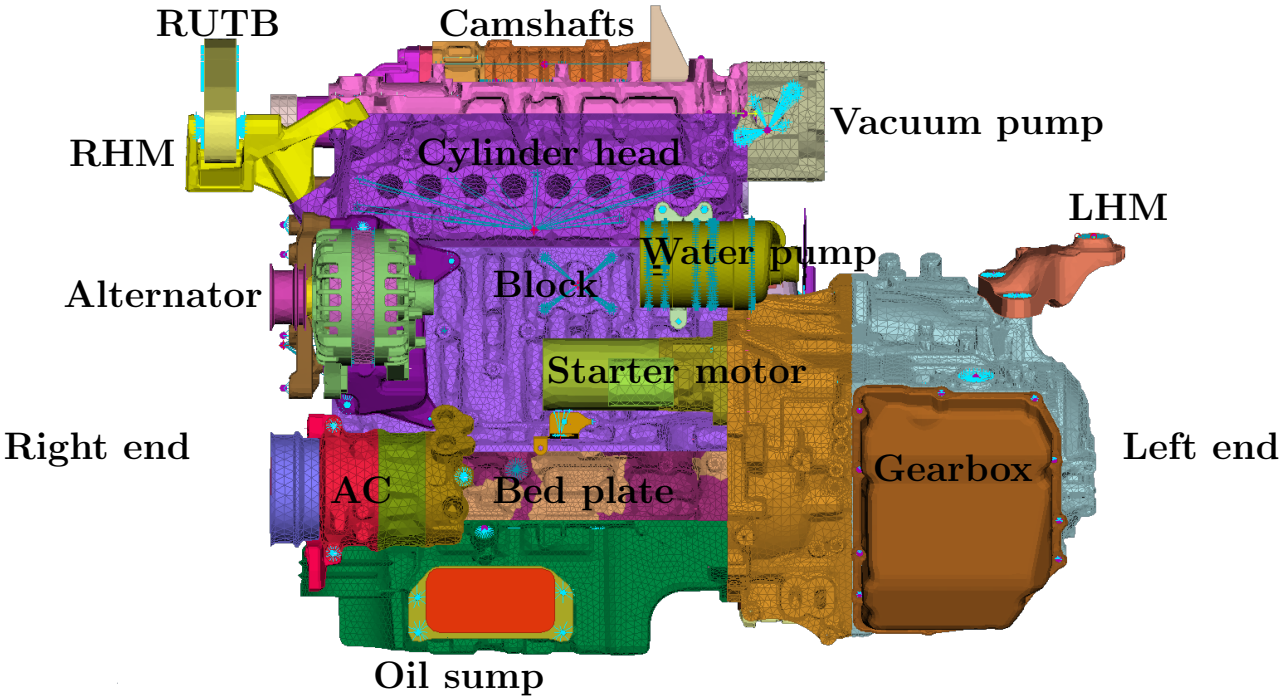

(b) The back side of the engine labelled with main parts.

Figure 2.1: The front and back side of the engine, respectively, with main parts labelled on top of or near the part itself.

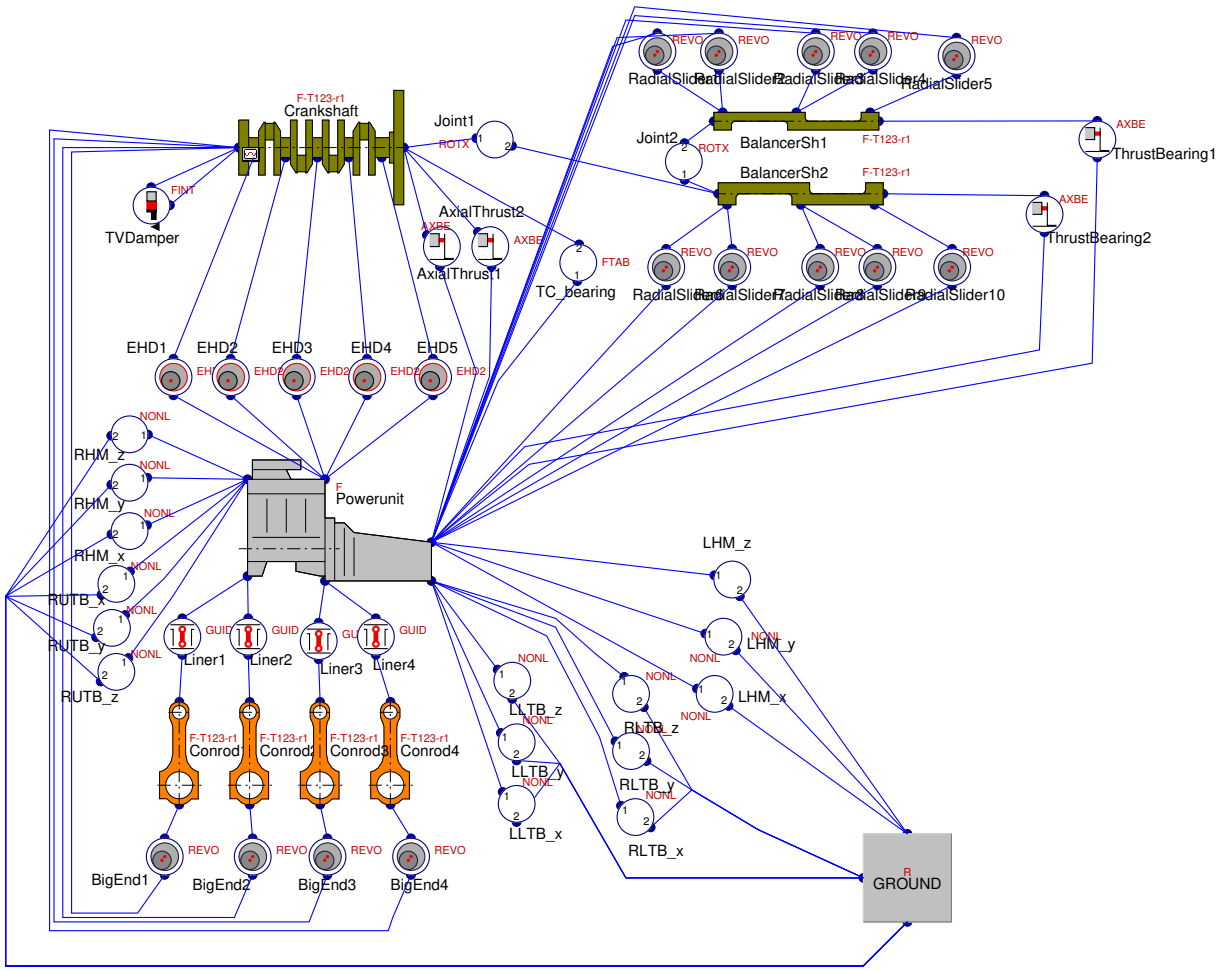

Figure 2.2: Schematic illustration of the multibody dynamics model in AVL EXCITE.

3 Parameter study

A parameter study in two levels is performed using sensitivity analysis (SA). First a large number of possibly important parameters are identified in a screening assessment. The most influential of these will then be analysed in the second level where a detailed parameter SA is performed. The two levels of SAs are presented and described in detail below.

3.1 Theory

Assume a set of n number of input factors x for a system, $\boldsymbol{x} = (x_1, x_2, ..., x_{n-1}, x_n)$. A SA is a method to investigate how an output function of a system, f, relies on one or many input parameters in $\boldsymbol{x}$. Thus, the aim is to find the relationship between information going in and out of the system [14]. There are numerous methods to perform a SA, and the selection of such is important to yield the desired insight in the system behaviour.

To conduct a SA requires a model of the investigated system to be constructed. The purpose of the SA should be determined and the relevant parameters identified or selected. The SA may give insight in e.g. significant and insignificant influential parameters, interaction effects between parameters and optimal regions for the parameters. Computational cost, model nonlinearity or/and additivity and purpose of investigation are all basis of deciding a relevant SA method [14].

3.2 Parameter alteration

The alteration of the parameters consists of changes on mass, stiffness, clearance and various combustion strategies. The alterations are made in the following way:

Mass The alteration of mass has been conducted by changing the specified material density in the finite element model, prior to superelement generation, keeping all other variables constant. Although practically non-feasible, it allows the study of how only mass affects the performance without consideration of e.g. geometrical changes.

Stiffness The alteration of stiffness has been conducted by changing the specified material Young's modulus in the finite element model, prior to superelement generation, keeping all other variables constant. Although practically non-feasible, it allows the study of how only stiffness affects the performance without consideration of e.g. geometrical changes.

Bearing clearance The alteration of bearing clearance has been conducted by changing the specified bearing clearance in the elasto-hydrodynamic joint in the multi body dynamics set up.

Combustion strategies The alteration of combustion strategies has been conducted by replacing the specified pressure data for each cylinder in the multi body dynamics set up. The pressure data is computed using, to this project, external and unknown modelling scripts and are ordered from the same external part, with a requirement that they should be relevant and realistic. The strategies of interest in this project are the ignition retardation and the combustion duration.

3.3 Screening

A screening is performed changing one factor at a time (OFAT), where each parameter variation is ranked with a sensitivity metric (S) according to Equation (3.1) [15].

$$S_i = \frac{x_{i,\max} - x_{i,\min}}{f_{ref}} \frac{f(x_1, ..., x_i + \Delta x_i, ..., x_n) - f(x_1, ..., x_n)}{\Delta x_i} \\ \Delta x_i = |x_{i,\text{original}} - x_{i,\text{variation}}| \tag{3.1}$$

Subscript i represents the i:th parameter, n the number of parameters, x the parameters, f the target function and f_{ref} a reference value of the target function. This yields comparable non-dimensional numbers that relate the performance of each parameter variation to that of a reference.

For the screening $x_{i,\max} - x_{i,\min} = \Delta x_i$ is chosen, and equation (3.1) can be simplified into Equation (3.2) below.

$$S_i = \frac{f(x_1, ..., x_i + \Delta x_i, ..., x_n) - f(x_1, ..., x_n)}{f_{\text{ref}}} \tag{3.2}$$

The OFAT method is typically used when performing a so called local sensitivity analysis (LSA). Note that for a LSA choosing $x_{i,\max} - x_{i,\min} = \Delta x_i$ is considered a large change, whereas it is recommended to select a small change in each parameter [15], as a rule of thumb 1 % is recommended [14]. The deliberate disregard of those recommendations are made on the basis that a small change would probably not affect the results in a considerable amount and that the method is rather used as screening meant to capture the general behaviour of the target function with respect to the parameters rather than the local behaviour.

The target function f is chosen to be the two worst combinations of node and degree of freedom regarding the PAPR factor in the baseline configuration. This occurs for vertical acceleration in the RHM and in the RLTB. For the same two nodes and direction the velocity is also evaluated to provide insight in how different quantities are related. Thus, f_{ref} takes these four values. The parameter alteration PAPR number is evaluated at these two locations and for the two quantities, and then related to its respective reference function f_{ref}.

According to [15] the LSA provides a low cost method to obtain information of influential parameters in a system. Even for a nonlinear case the system insight would be considerable. Compared to other SA methods the local variant is highly efficient with a required number of simulations equal to the number of investigated parameters plus one, as a baseline comparison. All above is assumed to apply also for the screening since using the same principal method to analyse the parameters.

3.3.1 Parameter selection

The parameters have been chosen based on available literature and the hypothesis of excitation and noise generation. The investigated parameters are presented in the list below:

Block & bed plate side mass and stiffness The mass-stiffness ratio from different parts of the engine to the mount is believed to influence the impulsive noise character. As a measure to study this, either the block & bed plate side material density were halved or the block & bed plate side Young's modulus were doubled. Note that only the block & bed plate side to the right of cylinder number 1 is altered, rather than the entire block & bed plate. This is due to consideration of implementation feasibility. See Figure 3.1 for visualisation of the parts altered.

Figure 3.1: The top right hand, in blue colour, and the bottom right hand, in orange colour, illustrate the block side and the bed plate side, respectively.

Crank shaft general stiffness The material Young's modulus were doubled for the entire crank shaft. This allows the study of only how the stiffness affects the impulsive noise character. In a real world implementation it would probably be needed to redesign the crank shaft and surrounding structures.

Crank shaft shank stiffness Due to the efficiency aspects of the downsizing of internal combustion engines the main bearing diameter, and thus the crank shaft stiffness, may not be possible to increase. Therefore beneficial consequences from modifying the crank shaft shank stiffness on the impulsive noise character were investigated. The material Young's modulus for the shanks were doubled. This is done to study only stiffness effects. However, the shanks would probably have to be redesigned in a real world implementation. The crank shaft shanks can be seen in Figure 3.2 below.

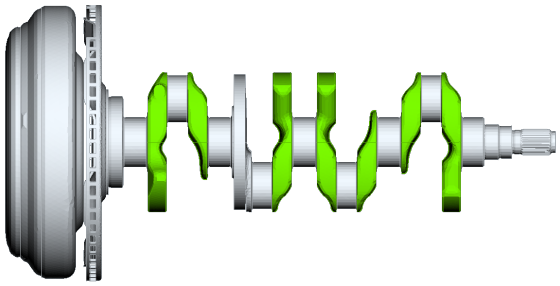

Figure 3.2: The crank shaft shanks, presented in green.

Cylinder head mass and stiffness The mass-stiffness ratio from different parts of the engine to the mount is believed to influence the impulsive noise character. As a measure to study this, either the cylinder head material density was doubled or the cylinder head Young's modulus was halved.

Main bearing clearance Part of the excitation of the engine structure is caused by the ignition in the cylinders. To study how the interaction between the rotating crank shaft and the power unit affects the impulsive noise character the main bearing clearance were halved, for all five main bearings.

RHM mass and stiffness Either the RHM material density was halved or the RHM Young's modulus was doubled to investigate if a lighter mount with higher natural frequencies would yield better noise characteristics in the cabin.

Combustion strategies In an internal combustion engine the combustion is controlled in multiple ways. This project has studied two of the main ones; (1) the combustion duration and (2) the ignition timing. In the descriptive list below these are explained. For a visual representation of the different combustion strategies and comparisons to the baseline case, please see Figure 3.3. All combustion strategies are altered with the ambition to keep the produced torque equal. Note that for the screening all altered

pressure data are produced only for an engine speed of 1500 rpm, however implemented and used to virtually drive the engine model throughout the engine speed range. Thus, the combustion strategies alterations can only be compared to each other and the baseline set up at that same rotational speed, called *standard* or *STD* below.

Ignition retardation The ignition timing is delayed in relation to the crank shaft angle, meaning that the combustion will start at a later crank shaft angle. This results in lower peak pressure, which is believed to be beneficial for the impulsive noise. The retardation is set to a reasonable maximum corresponding to what is believed as possible to physically implement.

All cylinders The ignition retardation is implemented in all cylinders.

Cylinder number 1 The generation of impulsive noise character is believed to be closely linked to the ignition in cylinder number 1. The retarded ignition timing is implemented only in this cylinder to see if a similar response in the RHM can be achieved with less of an alteration meaning fewer drawbacks, compared to if all cylinders had a retarded ignition.

Cylinder number 4 The retarded ignition timing is implemented in only cylinder number 4 to support or falsify the current hypothesis that the mass-stiffness ratios in proximity to cylinder number 1 is a cause of the impulsive noise character.

Combustion duration By changing the phase of the camshafts, it is possible to alter at what crank shaft angle the intake-/exhaust valves open and close. Doing so the combustion duration is altered. An earlier valve opening corresponds to a prolonged combustion duration and a later valve opening corresponds to a shortened combustion duration.

The combustion duration is set to a reasonable minimum and maximum, for short and long duration respectively, that would still be believed as able to physically implement.

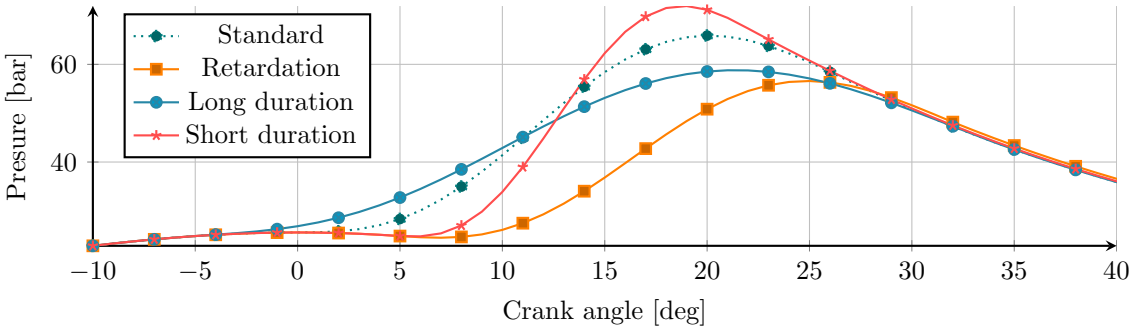

Figure 3.3: The four different pressure curves for the different combustion strategies in the parameter study. Engine speed 1500 rpm.

3.3.2 Results

The parameter evaluation is related to the baseline unless otherwise stated. One combination of direction, metric and mount point is further on referred to as an evaluation case. All calculated results are found in Appendix C.

In Figure 3.4 the time history data for the acceleration and the velocity in the vertical direction in the RHM for engine speed 2500 rpm is presented. The impulse after the ignition in cylinder number 1 is noticed. That impulse magnitude exceeds that of the other three cylinder ignition events. The impulsiveness is evaluated using the metrics presented in Section 2.5.

The PAPR results from the screening of the parameter study are presented below in Table 3.1. The presented data are, as stated earlier in Section 3.3, non-dimensional numbers of the relative difference compared to its respective reference. It is evident that the different evaluation cases have some ambiguities when compared. The fact that the sign differs in some of the cases, meaning that both improvements and disimprovements relative to the baseline are present, is regarded a significant one. Below follows a presentation and comparison

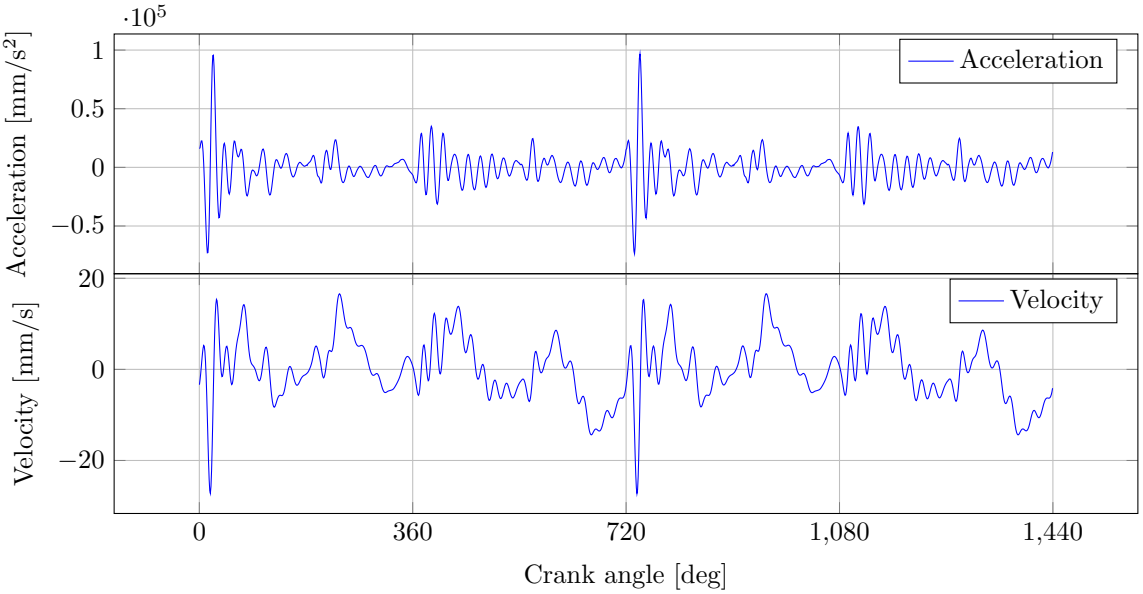

Figure 3.4: Time history data of vertical acceleration and velocity in the RHM during two full revolutions of the crank shaft. Engine speed 2500 rpm.

of the results from the evaluation of impulsive noise character for each case. For the spectrograms and the subjective listening the vertical velocity signal in the RHM has been used.

Table 3.1: The screening sensitivity results. The scale relates to the respective baseline value.

Parameter	**Scale**	**Acceleration**		**Velocity**	
		$\boldsymbol{S}_{\mathrm{RHM,z}}$	$\boldsymbol{S}_{\mathrm{RLTB,z}}$	$\boldsymbol{S}_{\mathrm{RHM,z}}$	$\boldsymbol{S}_{\mathrm{RLTB,z}}$
Block & bed plate side mass	0.5	0.025	0.135	0.248	0.147
Block & bed plate side stiffness	2	0.025	0.138	0.248	0.140
Crank shaft general stiffness	2	0.185	0.030	0.176	−0.020
Crank shaft shank stiffness	2	0.050	0.011	0.097	0.087
Cylinder head mass	2	−0.034	−0.016	−0.025	0.040
Cylinder head stiffness	0.5	0.032	−0.151	0.067	−0.040
Main bearing clearance	0.5	0.066	−0.035	0.050	−0.027
RHM mass	2	−0.002	0.000	−0.029	0.007
RHM stiffness	2	0.034	−0.008	−0.038	0.007
Cylinder no. 1 retardation	-	0.105	0.016	0.198	0.104
Cylinder no. 1-4 retardation	-	0.009	0.121	0.154	0.222
Cylinder no. 4 retardation	-	−0.046	−0.008	−0.022	−0.067
Combustion duration					
Long	-	0.323	0.134	0.538	0.370
Short	-	−0.320	−0.632	−0.505	−0.481

In Figure 3.5 the spectrogram for the baseline is presented. To aid the understanding the modulation is visualised in Figure 3.6. In the approximate frequency range 0 Hz to 250 Hz, further on referred to as the *low frequency region*, the largest velocity levels are generated. These low frequencies is characterised by a combination of low sensitivity of the human hearing as well as a non-distinct modulation behaviour. In combination this makes this area in the spectrogram relatively unimportant regarding the impulsive noise character (but will however play a big role in the general noise levels generated). At approximately 800 Hz large velocity levels are modulated with the engine half order, appearing after the ignition in cylinder number 1. This region is believed to give rise to the impulsive noise character in the vehicle cabin, and it is further on referred to as the *main impulsive region*. Note the less pertinent, by cylinder number 1 half order modulated, regions at slightly above 1000 Hz and at approximately 1400 Hz. These are in combination called the *high*

frequency bonus regions. Between the low frequency region and the main impulsive region there appears to be a first order modulated noise. The character however differs, and they are in fact two separate regions modulated at the engine half order, originating from the ignition in cylinder number 3 and 2. This region is referred to as the *middle region*.

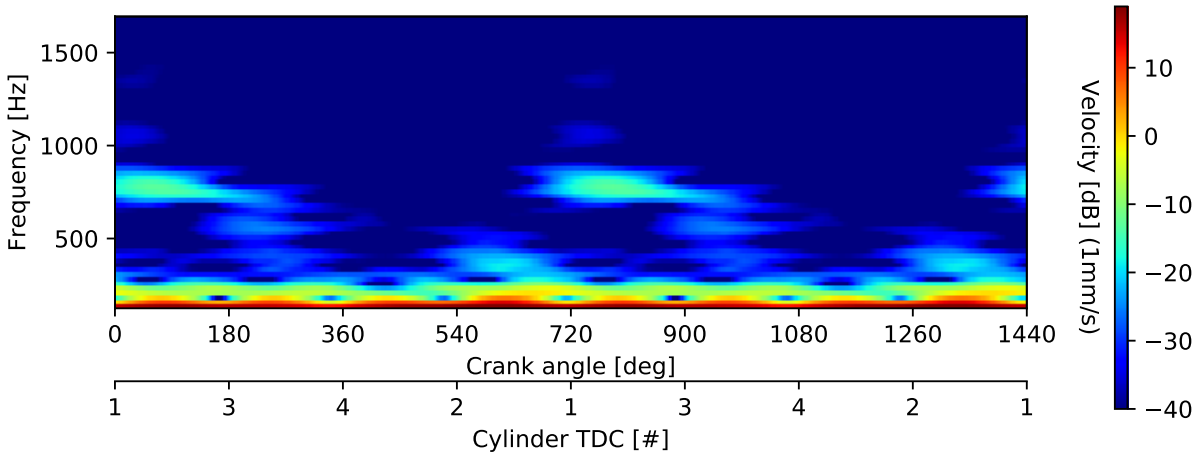

Figure 3.5: Spectrogram of vertical velocity at the RHM, simulated during two engine cycles. Engine speed 1500 rpm. Baseline configuration. The time instances for cylinder TDC are outlined at the bottom.

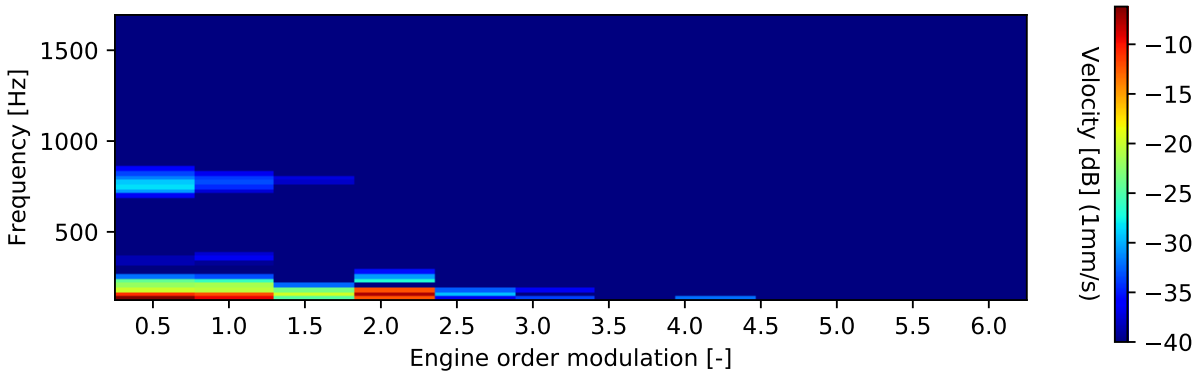

Figure 3.6: Modulation of vertical velocity at the RHM, simulated during two engine cycles. Engine speed 1500 rpm. Baseline configuration.

The PAPR data in Table 3.1 for the block & bed plate side mass and stiffness indicate that the two parameter alterations yield similar performance improvements. Figures 3.7 and 3.8 show spectrograms of velocity at the RHM. According to the PAPR data this is the evaluation case with the most significant improvement, almost four times better than the baseline. The overall sound pressure estimate in Figure 3.21 reveals that, in general, the two parameter alterations are comparable to that of the baseline. It is only at higher engine speeds that the block & bed plate side mass has a larger sound pressure value than the baseline. Thus, the PAPR reduction does mainly stem from an impulsive reduction and not a RMS increase. The spectrograms agree with that the two parameter alterations perform similarly, however does not show a significant reduction in peak velocity level. The high frequency bonus regions are diminished. Apart from that, the two spectrograms are comparable with the baseline, see Figure 3.5. Note the coarse scale of the colorbar.

The informal listening indicates an indistinguishable sound characteristics between the two parameter alterations and that there only exists a very slight impulsive noise character reduction. The informal listening has thus a better resemblance with the spectrograms than with the PAPR data.

When comparing the crank shaft general stiffness and the crank shaft shank stiffness in the PAPR evaluation Table 3.1 shows the crank shaft general stiffness to yield a considerable improvement with respect to PAPR at the RHM whereas the crank shaft shank stiffness is predicted to have a less significant impact on the expected

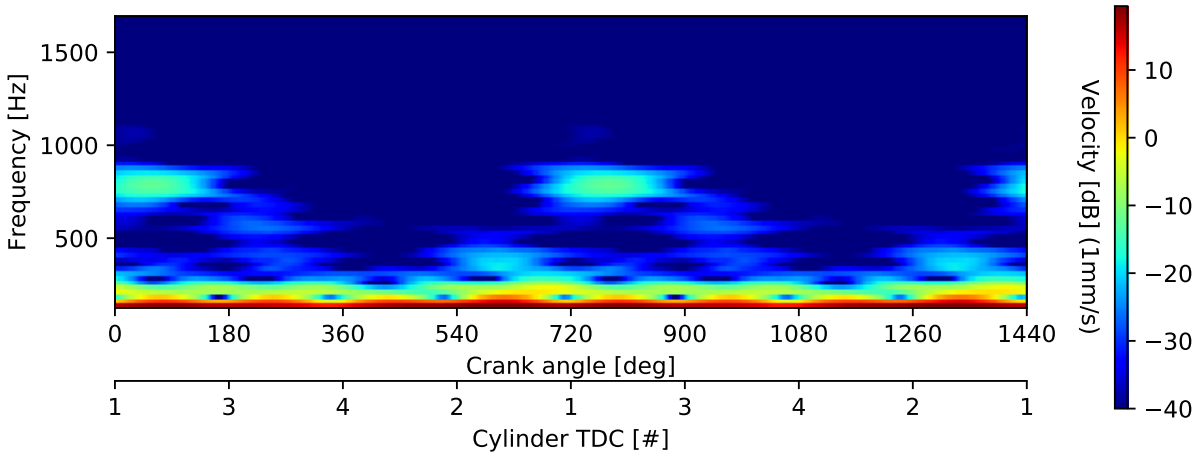

Figure 3.7: Spectrogram of vertical velocity at the RHM, simulated during two engine cycles. Engine speed 1500 rpm. Block & bed plate side mass configuration. The time instances for cylinder TDC are outlined at the bottom.

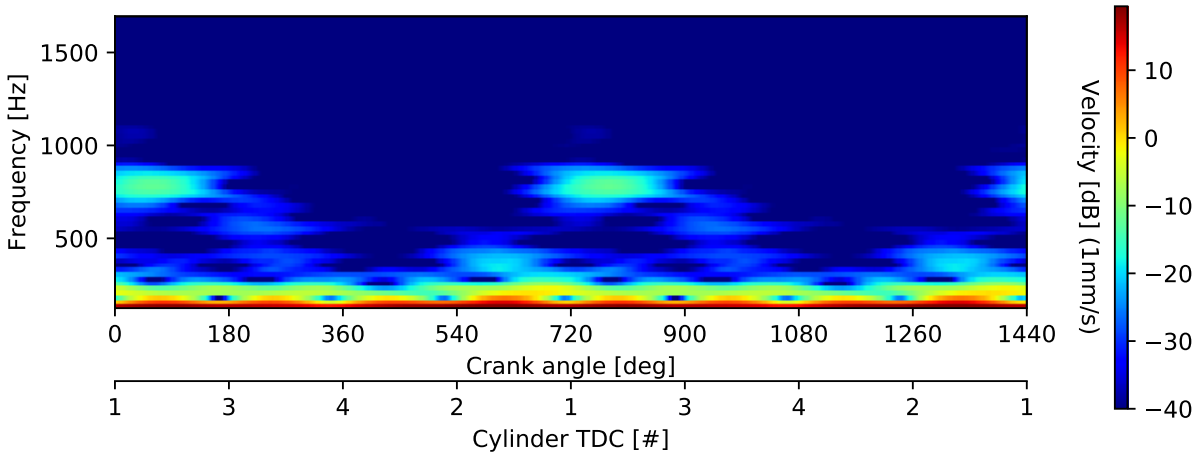

Figure 3.8: Spectrogram of vertical velocity at the RHM, simulated during two engine cycles. Engine speed 1500 rpm. Block & bed plate side stiffness configuration. The time instances for cylinder TDC are outlined at the bottom.

impulsiveness, in all evaluation cases apart from the velocity in the RLTB. Interestingly the spectrograms in Figures 3.9 and 3.10 does not only show a major reduction in impulsiveness as compared with the baseline, but also that the two parameter alterations are fairly similar in their velocity characteristics. The crank shaft general stiffness exhibits a lower magnitude for the main impulsive region and also a less cluttered middle region when compared to the crank shaft shank stiffness. In Figure 3.21 it is evident that both crank shaft stiffness alterations have a lower overall sound pressure level in the cabin, which makes the PAPR reduction even more significant. The two parameter evaluations manage to reduce the masking noise and reduce the expected impulsive noise even more, presumably resulting in a vastly improved sound characteristics in the cabin.

The informal listening indicates an improved sound with significantly less impulsive noise character. Since the sound files are normalised with the RMS-value only information about the sound characteristics may be found. Thus any conclusions regarding the lower overall sound pressure level in conjunction with less impulsiveness can not be drawn. All three evaluations of the impulsiveness indicate a major improvement, and both parameter alterations are regarded as interesting.

The cylinder head mass and stiffness have consistent results when comparing the PAPR evaluation in Table 3.1 and the spectrograms in Figures 3.11 and 3.12. The results indicate a sound signature with a high grade of

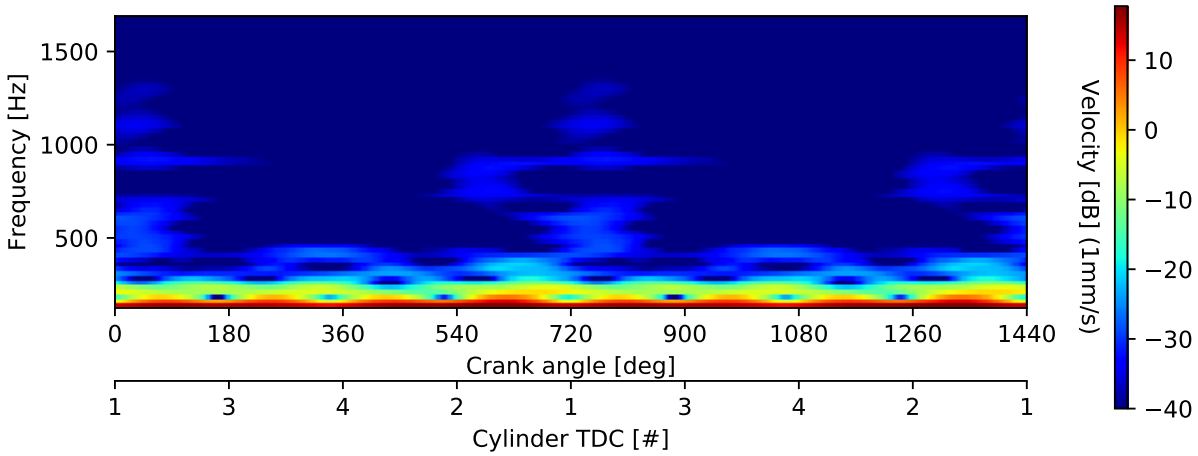

Figure 3.9: Spectrogram of vertical velocity at the RHM, simulated during two engine cycles. Engine speed 1500 rpm. Crank shaft general stiffness configuration. The time instances for cylinder TDC are outlined at the bottom.

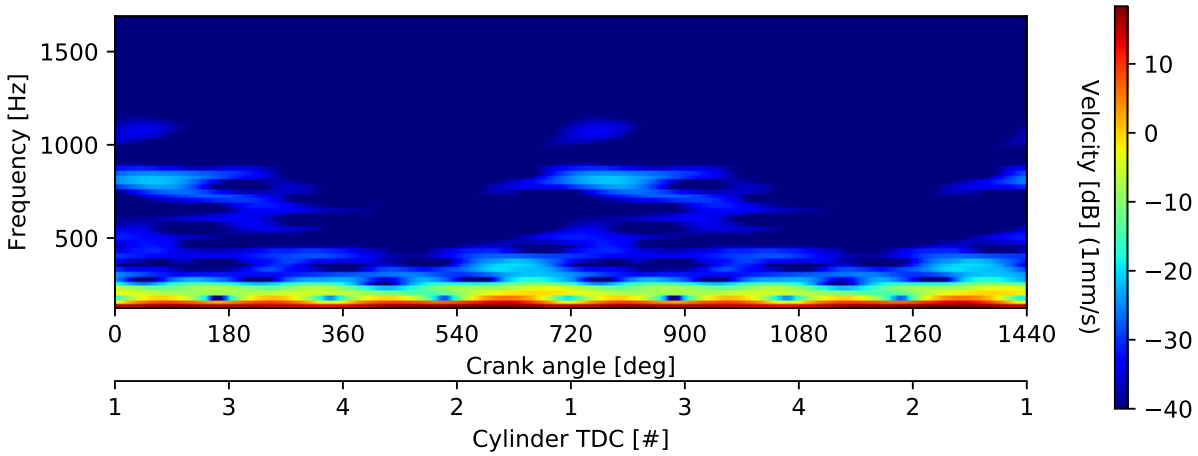

Figure 3.10: Spectrogram of vertical velocity at the RHM, simulated during two engine cycles. Engine speed 1500 rpm. Crank shaft shank stiffness configuration. The time instances for cylinder TDC are outlined at the bottom.

resemblance to the baseline. The overall sound pressure level estimate in Figure 3.21 is similar to that of the baseline.

The informal listening indicates a slight and minor impulsive noise character reduction. The alteration of the structural properties of the cylinder head is believed to be ineffective in the pursuit of lowering the impulsive noise character.

Based on the PAPR data in Table 3.1 the main bearing clearance has, when compared to the other parameter evaluations, a negligible impact on the impulsiveness. However, despite this the overall sound pressure level in Figure 3.21 shows that the reduction of main bearing clearance yields lower pressure levels than the baseline and thus potentially indicating a better sound signature despite the negligible PAPR data. The spectrogram in Figure 3.13 agrees with the PAPR data. Apart from a slight difference in velocity level in the high frequency region the spectrogram is similar to that of the baseline.

The informal listening indicates indistinguishable sound characteristics between the baseline and the reduced main bearing clearance.

In Figures 3.14 and 3.15 the velocity level spectrograms for the RHM mass and stiffness alterations are shown. The PAPR data in Table 3.1 indicate these two parameters to be insignificant, which is supported by the

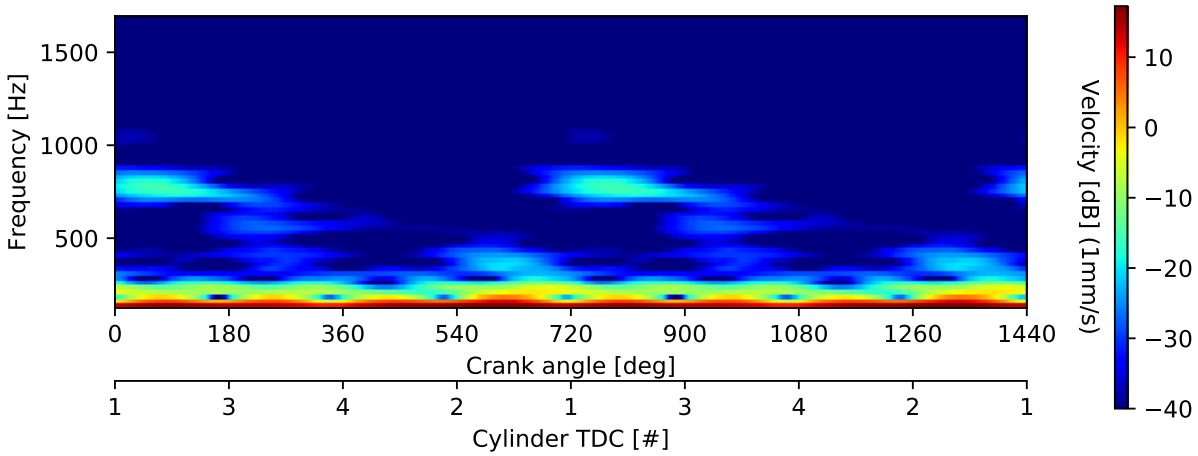

Figure 3.11: Spectrogram of vertical velocity at the RHM, simulated during two engine cycles. Engine speed 1500 rpm. Cylinder head mass configuration. The time instances for cylinder TDC are outlined at the bottom.

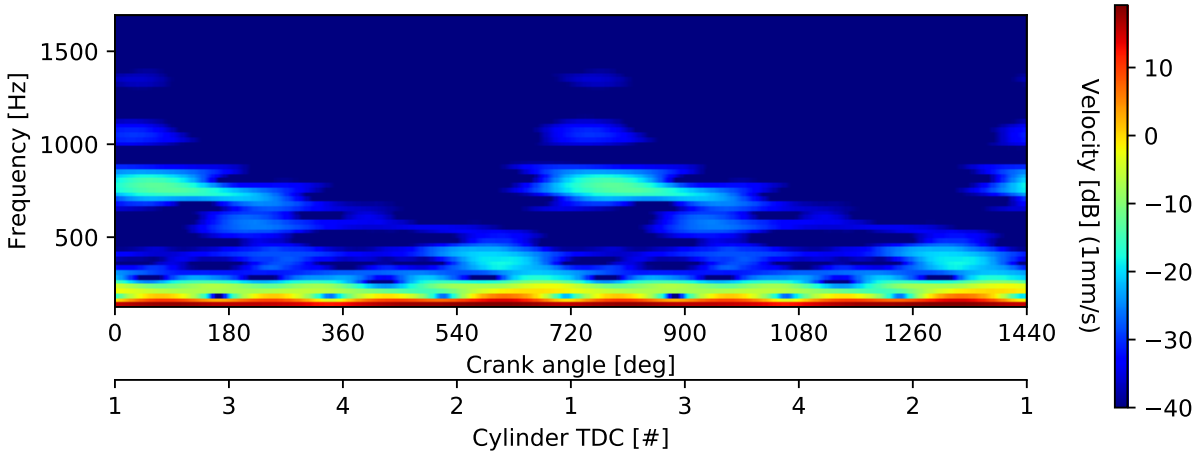

Figure 3.12: Spectrogram of vertical velocity at the RHM, simulated during two engine cycles. Engine speed 1500 rpm. Cylinder head stiffness configuration. The time instances for cylinder TDC are outlined at the bottom.

spectrograms. Note that the overall sound pressure level in Figure 3.21 for the two RHM alterations are similar to the baseline.

The retardation in cylinder number 1 shows a considerable improvement with respect to the PAPR, see Table 3.1. The same can be said for the retardation in all cylinders. Interestingly, for PAPR evaluated at the RHM, the retardation in only cylinder number 1 performs better than the retardation in all cylinders. It appears as if the impulse from cylinder number 1 is partly cancelled by the combustion- or mass impulse from one or several of the other cylinders. The velocity level spectrograms for the three different combustion strategies can be found in Figures 3.16, 3.17 and 3.18, respectively. These are almost seemingly identical, with only a slight improvement in the main impulsive region for the retardation in all cylinders between the three. That is not consistent with the PAPR presented in Table 3.1. All three spectrograms show a presumably improved sound characteristics based on the diminished high frequency bonus region and a nuance difference in the main impulsive region.

The informal listening agrees with the PAPR data and indicates a lot less impulsive noise character than the baseline.

The combustion duration stands out as the most significant parameter alteration in the PAPR evaluation of Table 3.1. This is further supported when looking at the spectrograms for short and long combustion duration presented in Figures 3.19 and 3.20. For short combustion duration velocity levels in the main impulsive

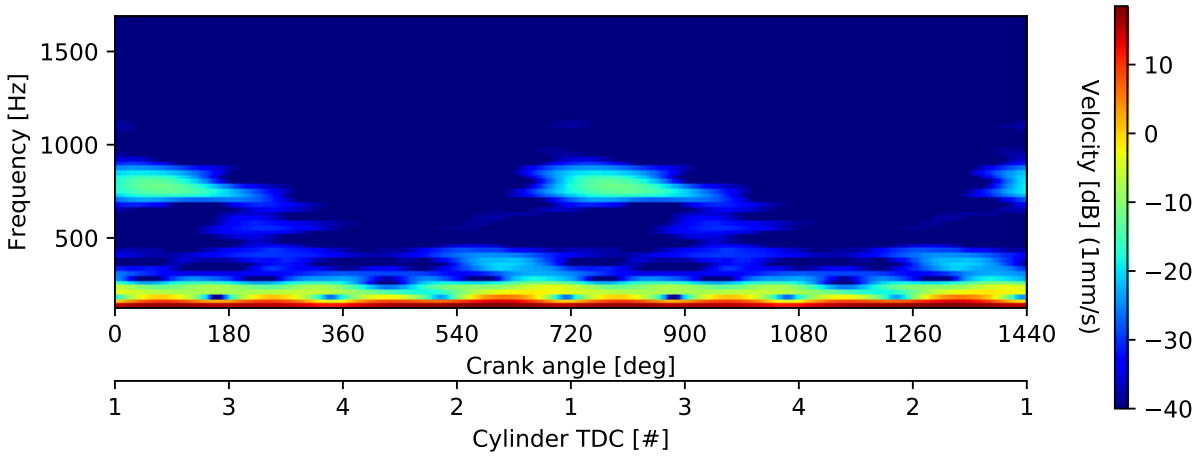

Figure 3.13: Spectrogram of vertical velocity at the RHM, simulated during two engine cycles. Engine speed 1500 rpm. Main bearing clearance configuration. The time instances for cylinder TDC are outlined at the bottom.

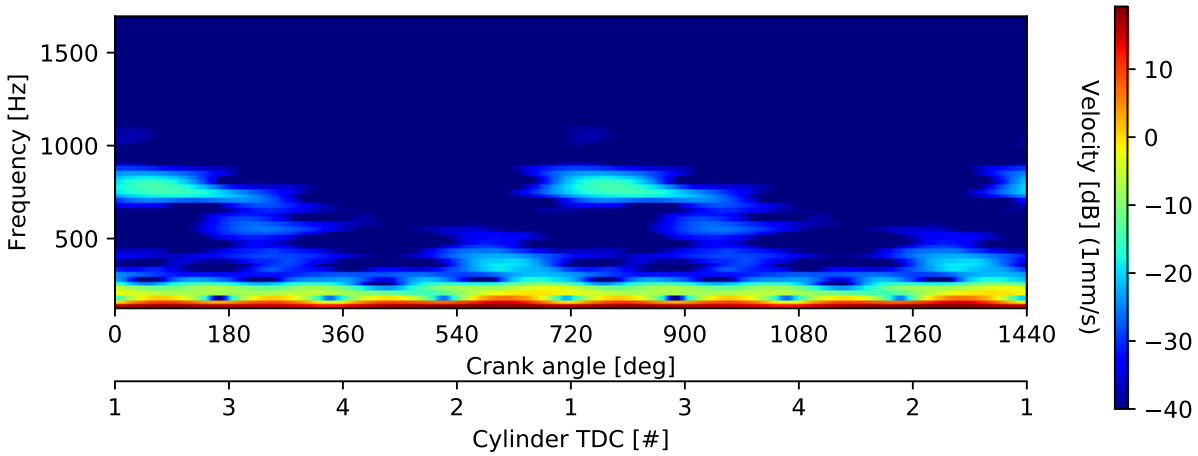

Figure 3.14: Spectrogram of vertical velocity at the RHM, simulated during two engine cycles. Engine speed 1500 rpm. RHM mass configuration. The time instances for cylinder TDC are outlined at the bottom.

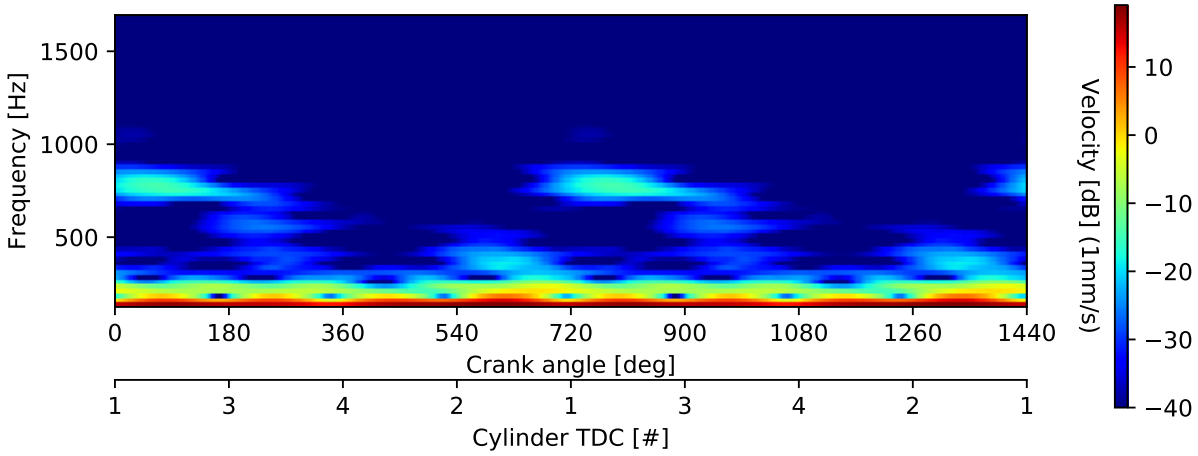

Figure 3.15: Spectrogram of vertical velocity at the RHM, simulated during two engine cycles. Engine speed 1500 rpm. RHM stiffness configuration. The time instances for cylinder TDC are outlined at the bottom.

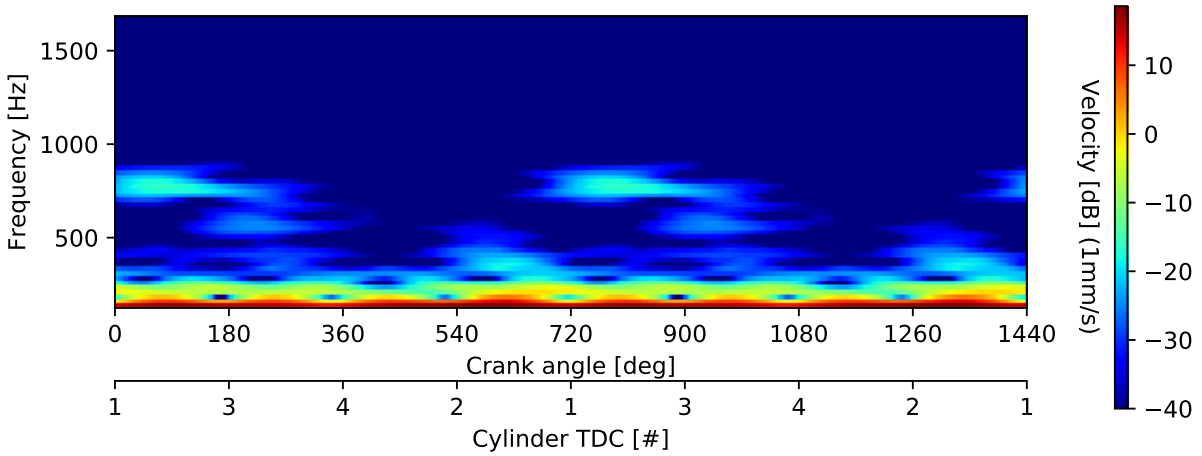

Figure 3.16: Spectrogram of vertical velocity at the RHM, simulated during two engine cycles. Engine speed 1500 rpm. Ignition retardation in cylinder number 1 combustion strategy configuration. The time instances for cylinder TDC are outlined at the bottom.

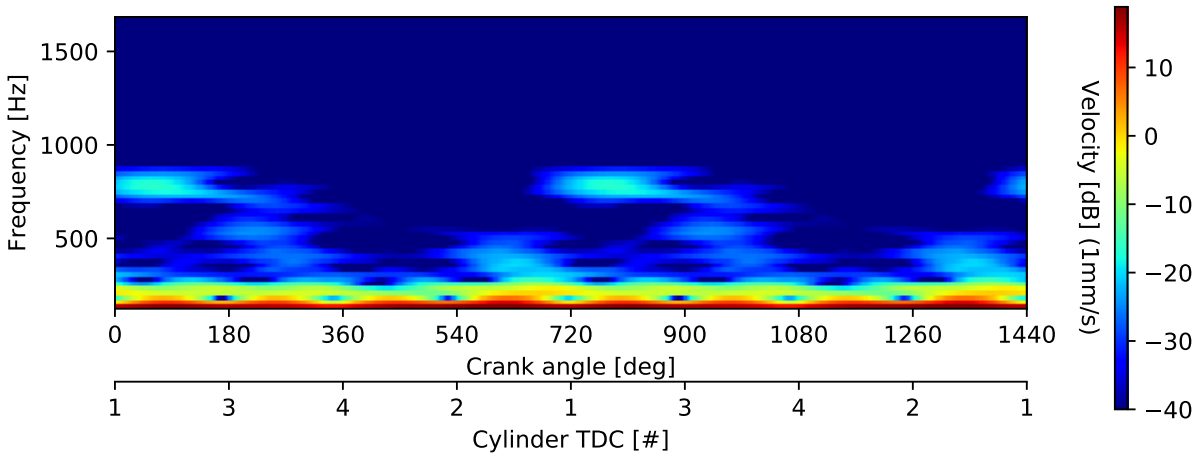

Figure 3.17: Spectrogram of vertical velocity at the RHM, simulated during two engine cycles. Engine speed 1500 rpm. Ignition retardation in all cylinders combustion strategy configuration. The time instances for cylinder TDC are outlined at the bottom.

region are increased, as compared to the baseline. The same can be said for the high frequency bonus region. Furthermore, the short combustion duration introduces a completely new half order modulated sound region, at approximately 1500 Hz. It seems to originate from the ignition in cylinder number 4. The short combustion duration is believed to have a very predominate impulsive noise character. The results for the long combustion duration has no significant half order modulated velocity levels at all. Significant velocity magnitudes remain only in the low frequency region. Based on the spectrogram this parameter alteration is believed to hardly have any impulsive noise character.

The informal listening supports these conclusions. The short and long combustion duration has the largest and lowest impulsive noise character, respectively, among all alterations. All evaluation metrics correlate and it may be concluded that the combustion duration is a highly relevant parameter for the impulsive noise character of the internal combustion engine.

When investigating the three different combustion strategies a simplified model of calculating pressure data was used. In Table 3.2 the mean torque of the different combustion strategies are presented, alongside with the measured pressure data in the baseline to verify the accuracy of the calculated pressure data. The seven different mean torques are approximately identical, with a maximum deviation of 4.5% from the measured baseline values.

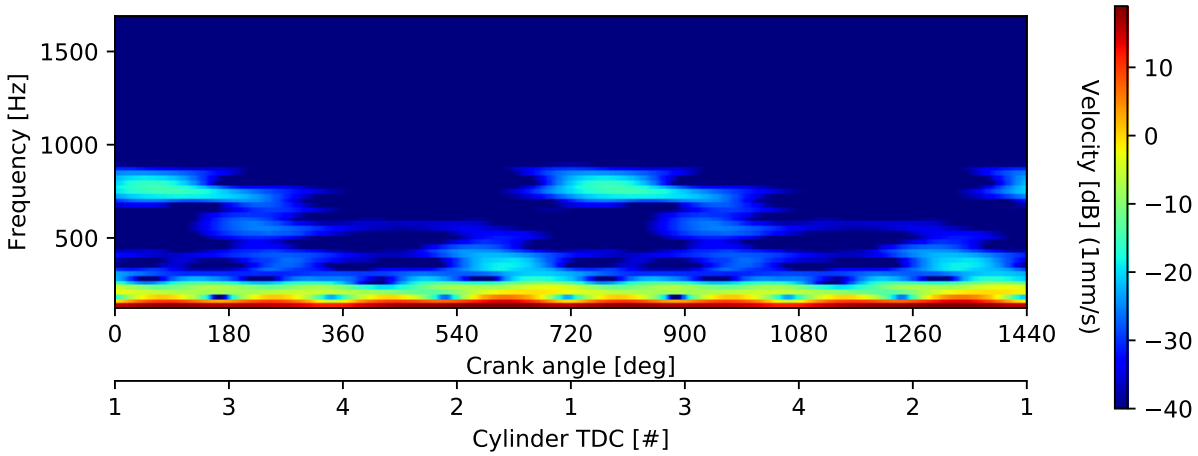

Figure 3.18: Spectrogram of vertical velocity at the RHM, simulated during two engine cycles. Engine speed 1500 rpm. Ignition retardation in cylinder number 4 combustion strategy configuration. The time instances for cylinder TDC are outlined at the bottom.

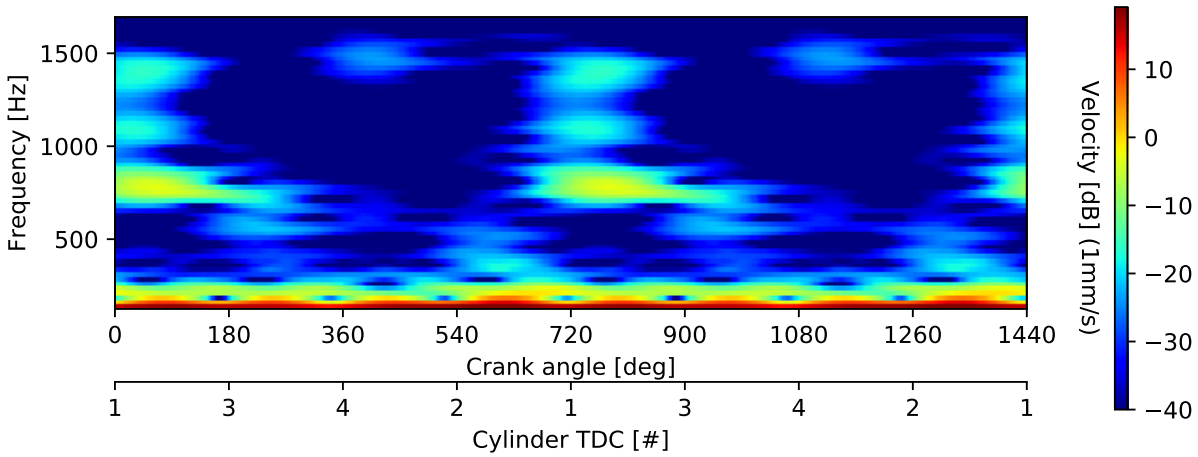

Figure 3.19: Spectrogram of vertical velocity at the RHM, simulated during two engine cycles. Engine speed 1500 rpm. Short duration combustion strategy configuration. The time instances for cylinder TDC are outlined at the bottom.

Table 3.2: The different combustion strategies and their respective mean torque.

Combustion strategy	**Mean torque** (@ 1500 rpm) [N m]	**Deviation** [%]
Baseline	224.7	-
Standard	224.3	0.18
Short combustion duration	226.4	0.76
Long combustion duration	219.9	2.1
Cylinder no. 1 retardation	221.9	1.2
Cylinder no. 1-4 retardation	214.7	4.5
Cylinder no. 4 retardation	221.9	2.1

An estimate of the total sound pressure level in the vehicle cabin is found in Figure 3.21. The total sound pressure levels for engine orders 0.5 to 20 have been accounted for. The rubber bushing frequency dependent stiffness data is imported into the model, and a forced response analysis is performed. A simplified transfer function between the engine mounts and the vehicle cabin is used. A-weighted sound pressure levels are presented. The graphs are used to get an overall estimate of the sound pressure in the cabin, but can not be used to identify the impulsive noise character. Moreover, due to the simplified transfer function, it can only be

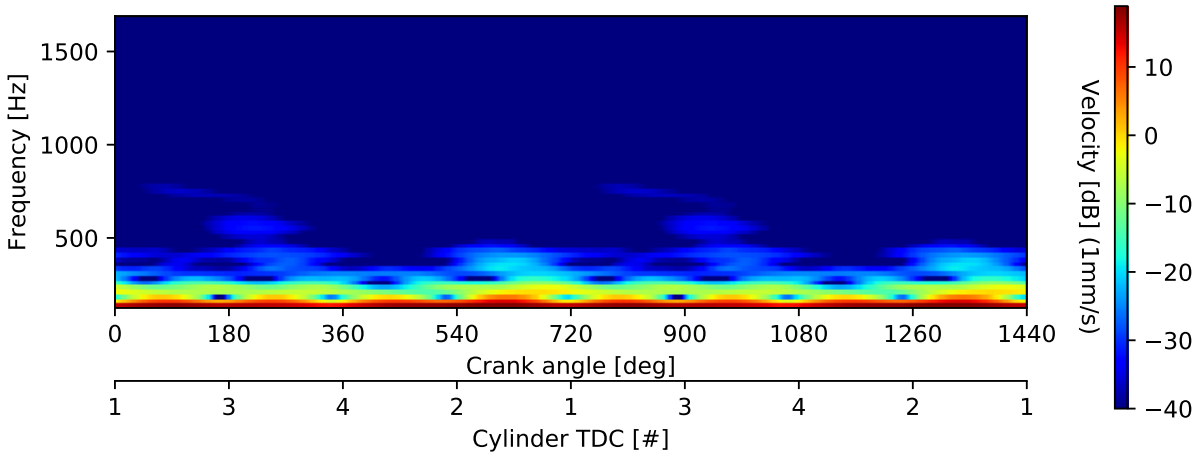

Figure 3.20: Spectrogram of vertical velocity at the RHM, simulated during two engine cycles. Engine speed 1500 rpm. Long duration combustion strategy configuration. The time instances for cylinder TDC are outlined at the bottom.

used as a relative comparison between the different cases, and not as an estimate of the actual sound pressure level. Note that the combustion strategies are not included since they are only valid at a single engine speed. The two crank shaft stiffness alterations stand out, especially the crank shaft general stiffness, and have at most approximately 1.5 dB lower overall sound pressure level than the baseline. That is a significant change.

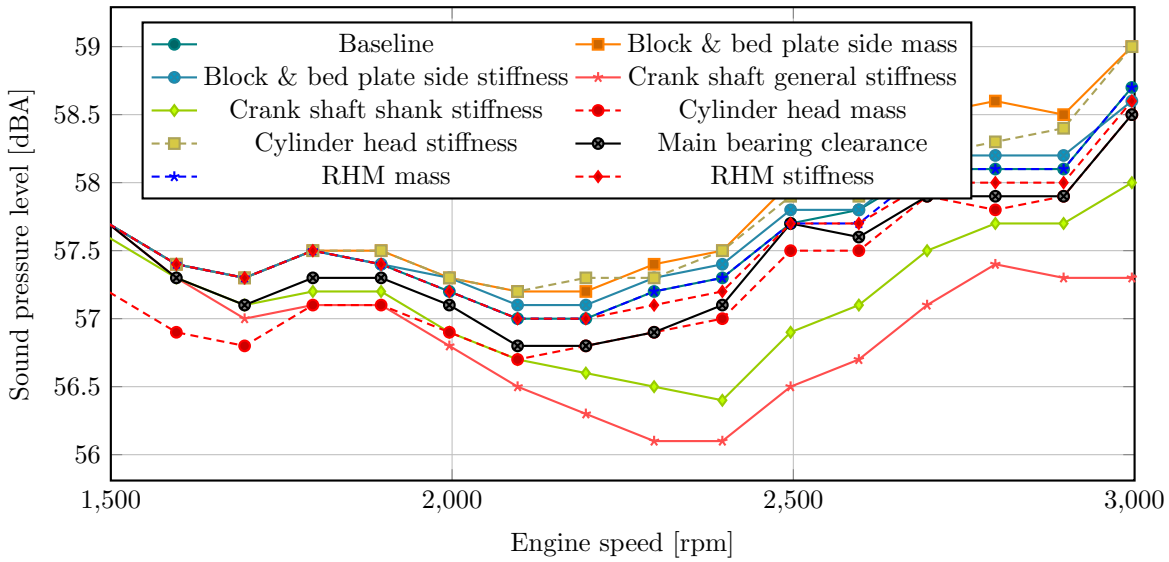

Figure 3.21: The sound pressure level overall estimate.

3.3.3 Discussion

The results differ between the two evaluation points. The data indicates that some parameter alterations have different signs in the different evaluation points indicating that a change may be both positive and negative, and thus not conclusive in if it would be beneficial or not in the pursuit of suppressing the impulsive noise character.

In [2] it was stated that the stiffness of the crank shaft (general stiffness), followed by the main bearing clearance, were the most important parameters to reduce the impulsive noise character. With respect to acceleration in the RHM and disregarding the combustion alterations, this is verified by the presented study. However, the

situation is different in the other evaluation cases and it is apparent that the selection of evaluation case has a big impact on the outcome. Based on all evaluation cases it might be argued that the block & bed plate side mass and the block & bed plate side stiffness have larger impact than the crank shaft general stiffness. However, the spectrograms do not support this conclusion but rather that they are fairly unimportant. Furthermore, the main bearing clearance has a relatively low impact in the other evaluation cases and it might be argued that its overall significance is quite low. Moreover, regarding the main bearing clearance it should be commented that the feasibility of implementation is low. The engine has to be able to operate and start in a broad range of conditions and performing a cold start in freezing temperatures may not be possible with a too tight clearance.

Some parameter alterations, such as the RHM mass and RHM stiffness, have negligible difference relative to the baseline, but may nevertheless play an important role by affecting the transfer of vibration to the cabin. According to its spectrogram that is however not the case. The informal listening does not agree with either the PAPR data or the spectrograms, as it indicates a lowered impulsive noise character.

Some parameter evaluations show both PAPR and velocity level spectrograms that suggest a significant influence on impulsiveness. It is apparent that the alteration of the combustion duration is a highly efficient way to reduce the PAPR. That holds true for all four evaluation cases. It is the most significant parameter in all evaluation cases, except that for acceleration in the RLTB, in which it is still the fourth best parameter.

Comparing the combustion strategies, it is interesting to see that an equally large difference in combustion duration (long duration versus short duration) does not yield an equally large impact on the PAPR. That is particularly true for acceleration calculated at the RLTB. It is furthermore highly interesting to see that, presumably, the impulse from cylinder number 1 is slightly cancelled by one or several of the other cylinders.

Some spectrograms differ clearly from the baseline and any conclusion based on these could be made with confidence. Some other spectrograms are seemingly identical, or very similar, to the baseline and each other and due to the relatively coarse colorbar scale conclusions based on these should be made with caution.

The overall sound pressure level, and thus the masking of the impulsive noise character, is important to consider in the analysis of PAPR and velocity level spectrograms. Since the PAPR data is relating peaks to the RMS of the same signal the inclusion of the overall sound pressure level is crucial to understand the PAPR data correctly interpret it.

3.4 Detailed parameter analysis

The elementary effects method (EEM) as proposed by [16] is performed, yielding a pseudo-global sensitivity analysis (GSA). The method can be viewed as an extended LSA with a more intricate design and evaluation, utilising the same principal OFAT methodology as in the screening in Section 3.3.

The method is performed in the following steps:

1. Specify parameters, x_i, and their maximum and minimum values, $x_{i,\max}$ and $x_{i,\min}$, respectively.
2. Normalise the parameter values to the interval $[0, 1]$ in p evenly spaced partitions,

$$\left[\frac{p-p}{p-1}, \frac{p-(p-1)}{p-1}, \frac{p-(p-2)}{p-1}, ..., \frac{p-(p-(p-1))}{p-1}\right] = \left[0, \frac{1}{p-1}, \frac{2}{p-1}, ..., 1\right] \tag{3.3}$$

   E.g. with $p = 4$ the normalised parameter interval becomes $\left[0, \frac{1}{3}, \frac{2}{3}, 1\right]$.
3. Choose a base case by adding or subtracting, if below or above half of the parameter interval respectively, a fixed normalised perturbation Δ to a randomly selected value on each parameters partitioned interval.

$$\Delta = \frac{p}{2\,(p-1)} \tag{3.4}$$

   E.g. with $p = 4$ the fixed normalised perturbation becomes $\Delta = \frac{2}{3}$. The base case corresponds to the first row in Equation (3.6).
4. Create a trajectory by, in the same manner, adding or subtracting Δ to only one randomly chosen parameter that has not been changed yet. This corresponds to all but the first rows in Equation (3.6).

5. Calculate the elementary effect, EE, for the i:th parameter, x_i, as

$$EE_i = \frac{1}{f_{\text{ref}}} \frac{f(x_1, ..., x_i + \Delta, ..., x_n) - f(x_1, ..., x_n)}{\Delta} \tag{3.5}$$

6. Evaluate the mean of EE ($\overline{EE}$), the standard deviation of EE (SD), the mean of absolute EE ($\overline{|EE|}$) and the standard error of the mean EE (SEM).

The EE is in a strict technical form a local sensitivity metric, however by performing several EE calculations per parameter, by performing the method in several trajectories, it is possible to get a pseudo-global behaviour of the metric. In [15] it is said that the $\overline{EE}$, being the average elementary effect over the entire parameter space, can be interpreted as a global sensitivity measure.

The $\overline{EE}$ and $\overline{|EE|}$ is used to predict the parameters overall significance to the output. A high mean indicates an important parameter. The SD is used to identify nonlinear effects and interaction effects, meaning parameters that interact with other parameters and/or have a nonlinear behaviour to the output [14]. The SEM is regarded as a confidence interval for the mean EE [15].

For each trajectory a matrix of settings per evaluation run is set up. Each trajectory consists of $n + 1$ runs since all parameters have to be changed one at a time from a base case. In Equation (3.6) an example matrix of a trajectory is presented. Each row corresponds to a case set up, and each column corresponds to a parameter. Thus, the dimension of such a matrix is $[(n + 1) \times n]$, where n, as for the LSA, denotes the total number of parameters evaluated.

$$B = \begin{bmatrix} 2/3 & 1/3 & 2/3 & 2/3 \\ 2/3 & 1/3 & 0 & 2/3 \\ 0 & 1/3 & 0 & 2/3 \\ 0 & 1 & 0 & 2/3 \\ 0 & 1 & 0 & 0 \end{bmatrix} \tag{3.6}$$

Note that each row only differs on one position from the succeeding one, meaning that only one parameter change takes place between two consecutive runs. In Appendix A the sampling generation code is presented. The trajectory matrices are presented in Appendix B.

In the original EEM the choice of p should be even. In conjunction with the suggested $\Delta = \frac{p}{p(p-1)}$, this means that, since having to stay within the given parameter interval $[0, 1]$, when below 0.5 in the parameter range Δ will be added and when above 0.5 in the parameter range Δ will be subtracted. Note that choosing p even guarantees not ending up on exactly 0.5 in the parameter range.

In order to guarantee a better trajectory coverage it has been suggested by [17] to generate a significantly larger number of trajectories (M) than the selected amount, r, in the paper approximately 500 to 1000 ($M >> r$). The best r number of trajectories are selected as a subset of these trajectories based on a distance evaluation. The method is viewed as interesting, but due to time restrictions the extension to the original EEM will be left as a recommendation for future work. The method has been further developed by [18] to improve computational cost, however time is still not sufficient to allow for implementation.

In a completely strict sense the parameters may have different spacing [19], that is having different values of p, yielding different values of the fixed pertubation Δ. However in this analysis all parameter intervals are treated equally, apart from the combustion duration that could not be controlled and has a slight deviation compared to the other parameters. See Section 3.4.1 and Table 3.3 for more information regarding this matter.

The main advantage of the EEM is the relatively low computational cost. That is a key factor to enable a feasible study. The main disadvantage of the EEM is the inability to estimate individual interactions between parameters. The method only provides a general estimate of interaction effects [14]. The low computational cost is highly valued and is considered a main cause to the selection of the method.

For the detailed parameter sensitivity analysis only engine speeds of 1500 rpm to 3000 rpm have been considered to make computational time manageable. The range is selected as it is identified as the most relevant engine speed range.

3.4.1 Parameter selection

The selection of parameters to study in the detailed parameter sensitivity analysis is based on (1) the results in Table 3.1 in Section 3.3.2, (2) the feasibility of a real world implementation and (3) the possibility to study approximately the same type of response (e.g. halved mass and doubled stiffness). The selected parameters are:

Block & bed plate side stiffness The block & bed plate side stiffness has a high ranking, is considered as easy to implement and covers some of the effects a mass change would have.

Cylinder head stiffness The cylinder head stiffness has a medium ranking, however at the RLTB in Table 3.1, it has the best impact with respect to acceleration. It is considered easy to implement and covers some of the effects a mass change would have.

Crank shaft general stiffness The crank shaft general stiffness has a high ranking. At present date an implementation of the shank stiffness would be more feasible, however both are practically impossible to implement without a complete redesign of the crank shaft and thus the more open-minded general stiffness is chosen to better study stiffness in a general fashion.

Long combustion duration The combustion strategy to alter the duration is the best performing parameter change in the local sensitivity analysis. A shorter combustion duration yields bad results and a longer combustion duration has the opposite effect. The parameter change is considered easy to implement. The pressure data was generated for 1500 rpm, 2275 rpm and 3000 rpm and then interpolated by AVL EXCITE to fill in the intermittent intervals. The relative comparison between the long combustion duration and the three other parameter alterations is thus regarded valid even outside of the three specified pressure data speeds.

The parameter set up is presented in Table 3.3. Note the two different non-normalised ranges for the block & bed plate side stiffness. Due to the fact that the two structural components have a slight difference in their respective modelled material properties, that difference is accounted for throughout the EEM. Also note the non-uniformly distributed interval for the long combustion duration, meaning that the partition size differs. The pressure data is computed by a to this project external part and delivered as is. The spacing between the four partitions is thus accounted for by utilising different values on the pertubation Δ depending on the actual interval. This is not expected to impact the outcome of the study and is mentioned for full disclosure.

The four different combustion duration pressure curves are presented for one engine speed in Figure 3.22. The differences between the curves are seemingly fractional, however believed to have a large impact on the impulsiveness based on the results from the LSA, see Section 3.3.2. The pressure curves are calculated based on the premises that they should all perform the same nominal work. The duration is stated as two different figures; (1) how many crank shaft rotational angles it takes from the first ten percent to the last ninety percent and (2) how many crank shaft rotational angles it takes to complete the entire combustion event. When differentiating between the four pressure data curves, the second figure is chosen to simplify the presentation and understanding, although the first also differs between the pressure curves.

Table 3.3: The four selected parameters for the elementary effects method and their respective range and normalised pertubation Δ.

Parameter	**Normalised range**	**Non-normalised range**	**Δ**
Block & bed plate side stiffness	[0, 1/3, 2/3, 1]	[75, 100, 125, 150] [GPa] [70, $93\frac{1}{3}$, $116\frac{2}{3}$, 140]	2/3
Cylinder head stiffness	[0, 1/3, 2/3, 1]	[75, 100, 125, 150] [GPa]	2/3
Crank shaft general stiffness	[0, 1/3, 2/3, 1]	[210, 280, 350, 420] [GPa]	2/3
Long combustion duration	[0, 3/8, 6/8, 1]	[28, 31, 34, 36] [deg]	5/8 & 6/8

3.4.2 Results

The results from the elementary effects study are presented below. The PAPR of velocity and acceleration in vertical direction is calculated at the RHM and RLTB. Tables 3.4, 3.5, 3.6 and 3.7 present ten elementary

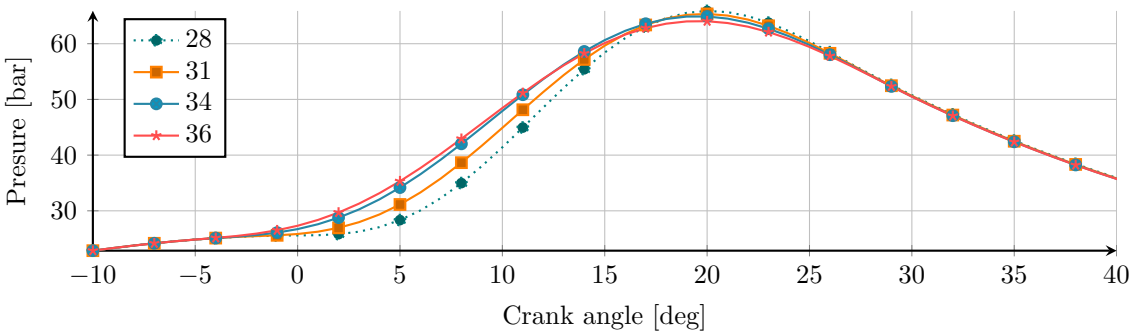

Figure 3.22: The four different pressure curves used for the long duration parameter. Engine speed 1500 rpm.

effects for each of the selected parameters.

In general the elementary effect calculated at the RHM exceeds that for the RLTB. It can be concluded that influence from the cylinder head structural properties is moderate.

Table 3.4: Cylinder head stiffness elementary effects.

Cylinder head stiffness											
		EE_1	EE_2	EE_3	EE_4	EE_5	EE_6	EE_7	EE_8	EE_9	EE_{10}
RHM	**Velocity**	0.00	-0.30	1.20	0.30	0.90	-0.90	1.35	0.45	-1.20	-1.20
	Acceleration	-0.45	0.60	4.05	-1.95	1.80	-0.75	2.70	1.80	0.90	-0.45
RLTB	**Velocity**	0.30	-0.45	-0.15	-0.15	-0.15	0.30	0.00	0.15	0.30	0.30
	Acceleration	-1.05	0.15	-1.35	1.20	-0.45	-0.90	-1.50	-1.65	-3.60	-3.30

Table 3.5: Block & bed plate side stiffness elementary effects.

Block & Bed plate side stiffness											
		EE_1	EE_2	EE_3	EE_4	EE_5	EE_6	EE_7	EE_8	EE_9	EE_{10}
RHM	**Velocity**	4.80	5.85	2.40	3.45	2.10	2.40	6.90	4.35	4.65	2.25
	Acceleration	2.25	1.20	2.40	2.40	2.25	3.45	1.95	4.05	1.95	3.00
RLTB	**Velocity**	-0.15	0.90	0.15	-0.60	-0.30	0.45	-0.15	0.45	1.05	0.45
	Acceleration	3.00	4.05	1.65	2.55	0.90	1.50	2.85	1.50	2.55	1.50

Table 3.6: Crank shaft general stiffness elementary effects.

Crank shaft general stiffness											
		EE_1	EE_2	EE_3	EE_4	EE_5	EE_6	EE_7	EE_8	EE_9	EE_{10}
RHM	**Velocity**	5.10	4.35	7.80	5.10	5.40	5.55	5.55	5.70	4.35	4.20
	Acceleration	13.05	4.50	13.65	13.65	15.45	5.85	15.45	5.10	1.80	6.90
RLTB	**Velocity**	0.30	-1.35	0.15	0.90	0.60	-1.20	0.90	-1.80	-1.20	-1.65
	Acceleration	4.20	7.20	3.60	2.55	3.75	3.30	3.00	3.00	8.85	4.50

Table 3.8 confirms, by comparing the $\overline{EE}$ and $\overline{|EE|}$ for the RHM and RLTB, that the RHM is a more important mounting point than the RLTB. Furthermore, regardless of evaluation case, the cylinder head stiffness is insignificant compared to the other parameters. The overall importance of the parameters are evaluated using the $\overline{EE}$ and $\overline{|EE|}$. It is clear that the most important parameters are the crank shaft stiffness and the combustion duration. Their respective ranking is dependent on the evaluation case, however the crank shaft general stiffness might be regarded as the overall most significant parameter. The block & bed plate side

Table 3.7: Long combustion duration elementary effects.

Long combustion duration										
		EE_1	EE_2	EE_3	EE_4	EE_5	EE_6	EE_7	EE_8	EE_9	EE_{10}
RHM	**Velocity**	5.33	5.47	6.24	4.67	5.73	4.67	5.87	5.20	7.04	3.84
	Acceleration	8.00	6.53	9.60	6.93	7.07	8.27	5.73	8.00	9.28	5.76
RLTB	**Velocity**	0.93	0.67	0.96	1.07	0.53	0.93	0.67	1.07	1.60	1.60
	Acceleration	5.73	-5.87	0.96	3.07	-1.20	-2.80	-0.93	-2.80	-2.08	-2.56

stiffness yields considerable improvements, however not at the same magnitude as the previously mentioned ones. The cylinder head is rejected as an effective way to reduce the impulsive noise character.

The SD is used to assess interaction- and nonlinear parameter effects. Table 3.8 shows that the SD at the RHM is larger compared to the RLTB and that may be regarded as that the coupling between the RHM and the rest of the engine is complex. Thus, the hypothesis that the mass-stiffness ratio between the cylinder head and engine mount, and base structure and engine mount, respectively, may be too simple.

Table 3.8 also shows that the crank shaft general stiffness has the largest or second largest SD in all evaluation cases. It may be concluded that among these parameters its interaction with other parameters and/or nonlinearity is the largest. In the same way the cylinder head is concluded to have the smallest interaction/nonlinear effect.

The combustion duration and the block & bed plate side stiffness does not stand out in the same way as the other two parameters in Table 3.8, apart from the one evaluation case looking at acceleration in the RLTB, where the combustion duration has a fairly large SD.

The SEM is to be regarded as a confidence in the results, where a large value indicates a high grade of uncertainty. Table 3.8 shows that a large magnitude SEM is calculated for the acceleration at the RHM and RLTB, for variation of the crank shaft general stiffness and combustion strategy, respectively. Thus, the results for these two evaluation cases may have to be regarded more approximate than for other cases.

Table 3.8: The evaluation of the elementary effects of vertical velocity and acceleration calculated at the RHM and RLTB for the four analysed parameters. $\overline{EE}$ is the mean of the EE, $\overline{|EE|}$ is the mean of the absolute EE, SD the standard deviation of the EE and SEM the standard error of the $\overline{|EE|}$.

EE evaluation									
		Velocity				**Acceleration**			
		$\overline{EE}$	$\overline{\|EE\|}$	**SD**	**SEM**	$\overline{EE}$	$\overline{\|EE\|}$	**SD**	**SEM**
RHM	**Cylinder head stiffness**	0.06	0.78	0.95	0.30	0.83	1.55	1.80	0.57
	Block & bed plate side stiffness	3.92	3.92	1.67	0.53	2.49	2.49	0.82	0.26
	Crank shaft stiffness	5.31	5.31	1.03	0.33	9.54	9.54	5.18	1.64
	Long combustion duration	5.41	5.41	0.90	0.28	7.52	7.52	1.34	0.43
RLTB	**Cylinder head stiffness**	0.05	0.23	0.27	0.08	-1.25	1.52	1.44	0.46
	Block & bed plate side stiffness	0.23	0.47	0.53	0.17	2.21	2.21	0.95	0.30
	Crank shaft stiffness	-0.44	1.01	1.10	0.35	4.40	4.40	2.04	0.64
	Long combustion duration	1.00	1.00	0.36	0.11	-0.85	2.80	3.32	1.05

The scatter plot in Figure 3.23 shows how the performance of the parameters are related to each other. A large SD value indicates significant interaction and/or nonlinerar effects. A large $\overline{EE}$ implies that the parameter has an important influence on the response. In other words, vertical position shows complexity and horizontal position shows importance.

Figure 3.23 shows the acceleration at the RHM calculated for varying crank shaft general stiffness to separate from the results for the other parameters. This is regarding both overall importance and interaction-/nonlinear effects. It becomes evident how most of the evaluation cases that concider variation in combustion duration

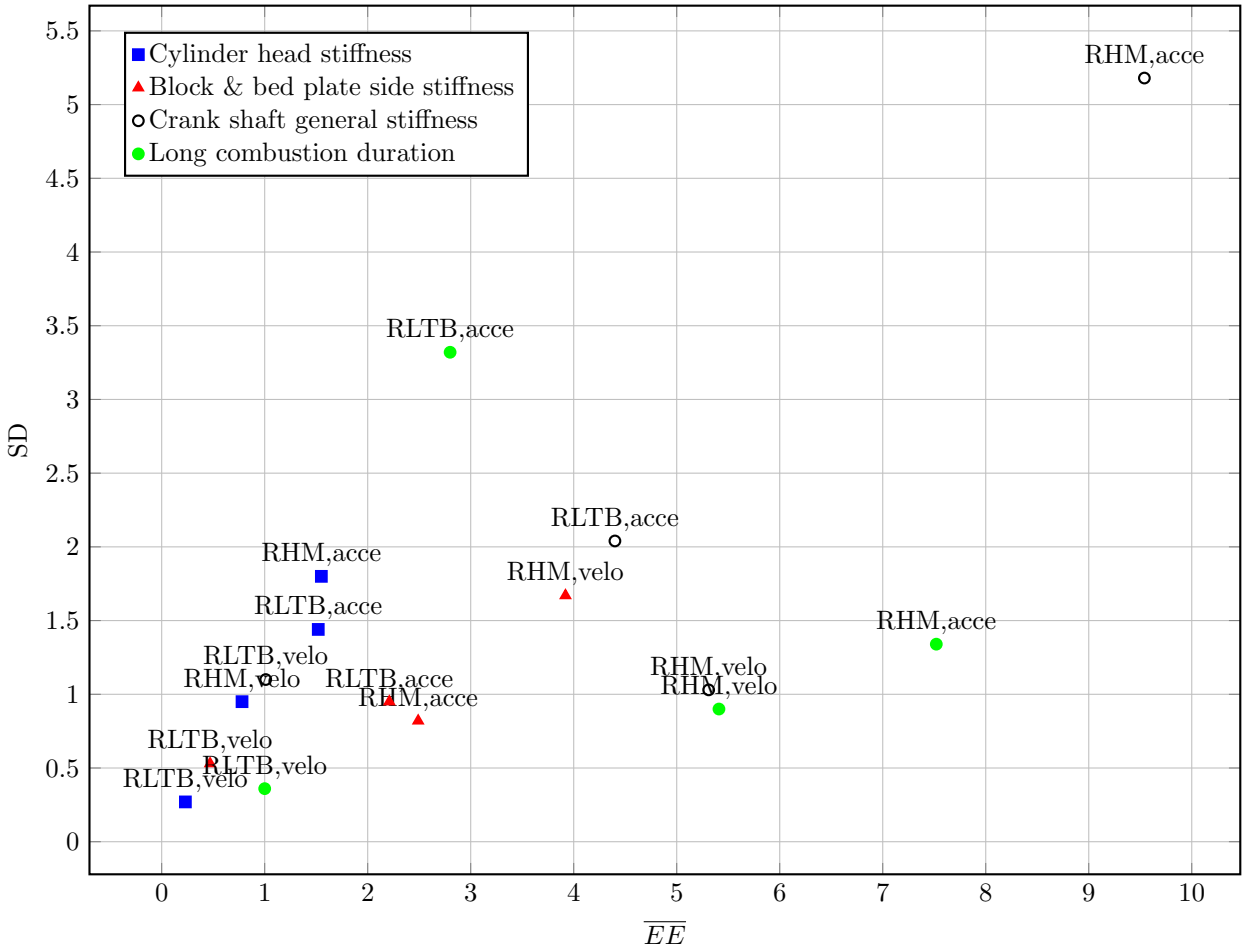

Figure 3.23: A visual representation of the relevance, $\overline{EE}$, and complexity, SD, for each parameter and evaluation case based on the results from the elementary effects method.

and the crank shaft general stiffness have a great importance on the system response. The opposite can be said about the cylinder head stiffness, which only has a moderate effect on the calculated velocity and acceleration at the considered locations. Regarding the complexity no general trend is found, however two points stand out; the crank shaft general stiffness regarding the acceleration in the RHM and the combustion duration regarding the acceleration in the RLTB.

3.4.3 Discussion

Based on the EEM additional information about the interaction- and nonlinear effects is found. The method provides insight in the importance of the different mounting points, where the RHM is found to be the main one regarding the impulsive noise character, supporting the working hypothesis at Volvo Cars.

The EEM supports many of the results and conclusions that were drawn based on the screening in Section 3.3.2. It is evident that there lies a great potential in impulsive noise character reduction in adjusting the crank shaft general stiffness and the combustion duration. The block & bed plate side stiffness may also be worth to consider as a way to further minimise the impulsive noise character. The cylinder head stiffness however is believed to have a negligible impact on the impulsive noise character, and the rejection in Section 3.3.2 is verified.

The large SD calculated for the the crank shaft general stiffness, implies that it is relevant to further study its impact on the model outcome throughout the entire parameter interval. Regarding the same parameter the SEM is relatively high, especially regarding the acceleration in the RHM, and thus the uncertainty in the

results is the largest for that parameter and evaluation case.

It is astounding that the seemingly minuscule combustion duration alterations, see Figure 3.22, results in such large changes in the outcome. It may be the easiest way, whilst still being a highly efficient countermeasure, to reduce the impulsive noise character, without any significant drawbacks from other perspectives.

For the EEM only stiffness alterations were considered for those parameters that also had a mass alteration in the screening. This was based on two arguments, (1) the modal behaviour is affected in similar ways by a stiffness increase as for a mass decrease and the stiffness was chosen based on the fact that (2) a stiffness requirement seems more natural in a design phase. Although the modal behaviour would be affected in similar ways, a stiffer component in interaction with another one, such as the crank shaft and the stationary engine, would also result in a difference in the coupling between the two.

4 Right hand mount design study

The possibility to mitigate impulsiveness by modifying the design of the RHM is studied. The design change is accomplished by connecting the RHM to different locations on the engine block or bed plate in order to emulate different types of RHM consoles. These connections were constructed by creating rigid body elements, by MSC NASTRAN called *RBE2*, at desired locations. Approximately 20 nodes at the surface were selected to emulate an attachment using a screw or bolt. This will make the approximately 20 nodes have dependent degree of freedoms all related to a single created independent node.

Between two RBE2 nodes, one located on the RHM and one located at a desired place on the engine block or bed plate, a simple beam element, by MSC NASTRAN called *CBAR*, was created. The beam was defined as a solid circular beam with a radius of 10 mm having the same aluminium material as used for the engine block.

Two different types of RHM stiffening was investigated:

1. The RHM fastening points were generally stiffened from also attaching them further down on the engine structure. Each original fastening point was thus comprised of four node attachment points; the two original ones (one on the RHM and one on the cylinder head) and the two stiffening ones (one on the RHM near the original node and one on the engine block or bed plate), all set to sustain load for all 6 DOFs.

2. The RHM was set up as a hinge at its original fastenings only restricting translational movement in the horizontal plane, and the other four DOFs restricted from the engine block or bed plate. This was achieved by only restricting horizontal translation at the original node fastening points and the remaining four DOFs set restricted for the RBE2s located on the engine block or bed plate. For this evaluation scenario a total of three RBE2 nodes were used; (1) the original one on the cylinder head only restricting horizontal translation, (2) the created stiffening one on the engine block or bed plate restricting all but horizontal plane translation and (3) the original one on the RHM with all six DOFs restricted.

4.1 Modelling set up

The RHM design changes were made for nine different cases. The set up opts to mimic a redesigned console and give insight in how it would be most beneficial to redesign the console. The nine different set ups are presented in Figure 4.2.

The cases were set up to investigate:

1. Where on the engine structure it would be most beneficial to take support.

2. Where on the RHM it would be most beneficial to give support.

3. What type of attachment on the RHM would be the most beneficial.

The nine test cases are described below, with reference and notation according to Figure 4.2.

Figure 4.2(a)/Left & right block support The three original fastenings are supported from the lower half of the engine block. Both the right hand side and the left hand side of the engine block are used for support.

Figure 4.2(b)/Left block support The three original fastenings are supported from the lower half of the engine block. Only the right hand side of the engine block is used for support.

Figure 4.2(c)/Block top support The three original fastenings are supported from the top of the engine block. The attachment location on the engine block is chosen close to the RHM attachment.

Figure 4.2(d)/Bed plate support The three original fastenings are supported from the bed plate. Both the right hand side and the left hand side of the bed plate are used for support.

Figure 4.2(e)/Cylinder head support Between the original fastening points on the RHM, near the cylinder head, one beam is giving support taken from near the centre of the engine block. In Figure 4.1(a) the RHM and the bar with connecting RBE2 are displayed from an alternative angle for better understanding.

Figure 4.2(f)/Suspension point support Between the original fastening points on the RHM, near the suspension point of the RHM, one beam is giving support taken from near the centre of the engine block. In Figure 4.1(b) the RHM and the bar with connecting RBE2 are displayed from an alternative angle for better understanding.

Figure 4.2(g)/Left & right block hinged support The three original fastenings are supported from the lower half of the engine block. Both the right hand side and the left hand side of the engine block are used for support. The RHM is hinged, meaning that horizontal plane translation is supported by the original fastening and the other DOFs are supported from the added beams.

Figure 4.2(h)/Block top hinged support The three original fastenings are supported from the top of the engine block. The attachment location on the engine block is chosen close to the RHM attachment. The RHM is hinged, meaning that horizontal plane translation is supported by the original fastening and the other DOFs are supported from the added beams.

Figure 4.2(i)/Bed plate hinged support The three original fastenings are supported from the bed plate. Both the right hand side and the left hand side of the bed plate are used for support. The RHM is hinged, meaning that horizontal plane translation is supported by the original fastening and the other DOFs are supported from the added beams.

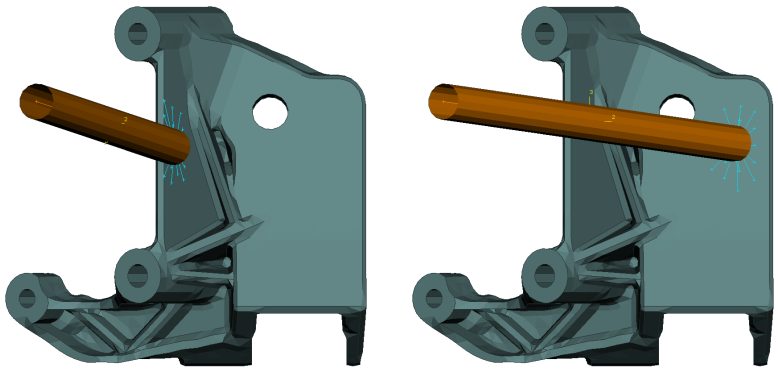

(a) The *cylinder head support* design case, where the support beam is located near the cylinder head on the RHM.

(b) The *suspension point support* design case, where the support beam is located near the suspension point of the RHM.

Figure 4.1: The two alternative attachment locations of the supporting beam on the RHM considered in the study.

Note that for the bed plate support, i.e. Figure 4.2(d), only a right hand side and left hand side set up was made. This was due to the difficulties with placing a beam without obstructing the crank shaft and not attaching it to close to the other beams yielding a stress concentration with possible unreliable results as a consequence.

4.2 Results

All calculated data from the design study are presented in Appendix D. The main purpose of the RHM is to sustain vertical loads, and thus the vertical component of the vibration is of extra interest. In Table 4.1 the PAPR sensitivity metrics for the vertical acceleration and velocity are presented. Note how almost all studied design cases yield a significant improvement as compared with the original RHM design. Also note how, in general, the improvement is larger for the velocity as compared with the acceleration, and thus being non conforming with the results in the parameter study where the situation is the opposite, see Table 3.1. Below

follows a presentation and comparison of the results from the evaluation of impulsive noise character for each case. For the spectrograms and the subjective listening the vertical velocity signal in the RHM has been used.

Table 4.1: The sensitivity analysis results for the vertical component of the acceleration and the velocity.

Parameter	$\boldsymbol{S}_{\mathrm{RHM,z}}$	
	Acceleration	**Velocity**
Left & right block support	0.269	0.521
Right block support	0.295	0.567
Block top support	−0.009	0.034
Bed plate support	0.352	0.508
Cylinder head support	0.276	0.508
Suspension point support	0.331	0.643
Left & right block hinged support	0.025	−0.042
Block top hinged support	−0.005	−0.029
Bed plate hinged support	0.329	0.315

Comparing the left & right block support (Figure 4.2(a)) and the right block support (Figure 4.2(b)) in Table 4.1 they do both provide a considerable improvement. This suggests that support further down on the engine structure is beneficial. The right block support performs slightly better than the left & right block support, however not by much, and it suggests that it could be interesting to optimise the support mounting point. The spectrograms in Figures 4.3 and 4.4 indicate a slight improvement in comparison the baseline. The high frequency bonus region is not present and the main impulsive region slightly recessed. The informal listening agrees with the PAPR data and indicates a reduced impulsive noise character.

Comparing results obtained in Table 4.1 between the left & right block support (Figure 4.2(a)) and right block support (Figure 4.2(b)) with the block top support (Figure 4.2(c)) and the bed plate support (Figure 4.2(d)) it indicates that it is not beneficial to have the RHM to take support from high up on the engine block. Moreover, the performance differences of taking support further down on the engine block or on the bed plate are fairly small and the results based on acceleration or velocity differ. Both support strategies are however efficient, regardless of evaluation metric. The previously discussed spectrograms for the left & right block support and right block support in Figures 4.3 and 4.4 and the two spectrograms for the block top support and the bed plate support in Figures 4.5 and 4.6, respectively, reveal a less pertinent change from the baseline than the PAPR data in Table 4.1 suggest. In conclusion the main impulsive region is recessed for the design cases where support is taken from far down on the engine, whereas the block top support design case performs only moderately better than the baseline. All stated conclusions above are supported and consistent with the informal listening.

The PAPR data suggest that the impulsiveness is suppressed most efficiently by stiffening the RHM near its mounting point to the car. That can be concluded by comparing results in Table 4.1 obtained for the suspension point support (Figure 4.1(b)) and the cylinder head support (Figure 4.1(a)). Note that the PAPR reduction obtained with one stiffening bar has a similar magnitude as that for the other cases. This indicates that the stiffening required to mitigate the impulsiveness is fairly modest, and corresponds mainly to an additional connection to the lower part of the engine structure. The spectrograms in Figures 4.7 and 4.8 both shows lower overall velocity levels than the baseline. In particular the suspension point support gives reduced velocity levels in the main impulsive region. Moreover the spectrograms support the PAPR on the advantage of supporting the RHM near the mounting point with the car. This is confirmed by the informal listening tests.

In Figures 4.9, 4.10 and 4.11 the spectrograms for the hinged design cases are shown. All three cases have a distinct main impulsive region and the general appearance is that all three perform worse than the baseline with respect to impulsiveness. The results from the informal listening are more consistent with the PAPR data in Table 4.1 indicating that the left & right block hinged support and the block top hinged support are worse than the baseline, and that the bed plate hinged support improves the sound characteristics of the engine. A modal analysis was performed for the three hinged cases, revealing that the used method appeared to not behave as desired.

4.3 Discussion

The PAPR data suggest that it would be highly beneficial for the RHM to take support on the engine structure. That support should be taken relatively far down on the engine block or bed plate, as extra support from high up on the engine block does not seem to provide any advantages regarding the impulsive noise character. That claim is however not fully supported by the spectrograms, where relatively minor changes are exhibited and the drastic changes shown in the PAPR data are not present. A more consistent result between the PAPR and the spectrograms are shown from some parameter alterations in the screening in Section 3.3.2, and it may at least be assumed that the redesign of the RHM is not the most efficient way to reduce the impulsive noise character from the internal combustion engine. An overall increase of sound pressure level may also lead to a greater masking of the impulsiveness, possibly explaining the seeming ambiguities between the PAPR and the spectrograms. The informal listening is consistent with the PAPR data and suggests that the redesign would be beneficial.

Based on the unexpected PAPR data and the suspicious modal behaviour the hinged design cases may not have been set up correctly. The other data suggest that it would be beneficial to take vertical load from further down on the engine structure, however by looking at the results in Table 4.1 for the left & right block hinged support (Figure 4.2(g)), the block top hinged support (Figure 4.2(h)) and the bed plate hinged support (Figure 4.2(i)) the first two result in a more impulsive vibration signal at the mounting point. The third design case performs well, but in combination with the other two the results are questionable and it seems as if the modelling set up did not achieve what was intended.

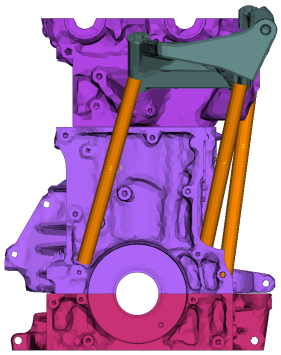

(a) Left & right block support. The RHM stiffened from the engine block, with support from both right and left part.

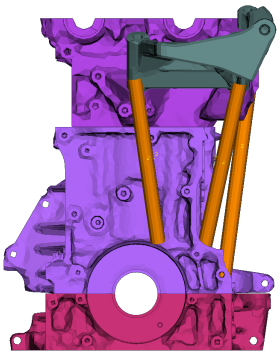

(b) Right block support. The RHM stiffened from the engine block, with support from mainly the right part.

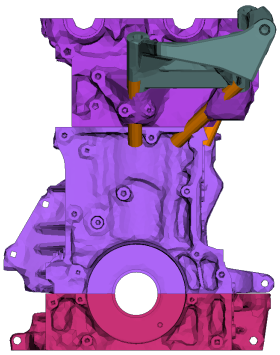

(c) block top support. The RHM stiffened from the top of the engine block.

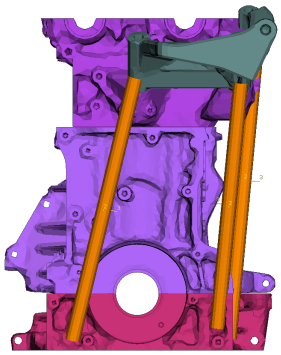

(d) Bed plate support. The RHM stiffened from the bed plate.

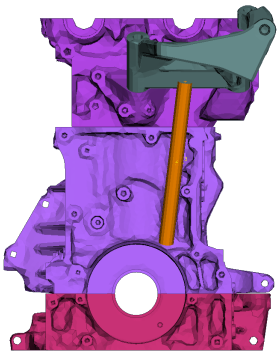

(e) Cylinder head support. The RHM stiffened from the block. Bar attachment located near the cylinder head, far away from the suspension point of the RHM.

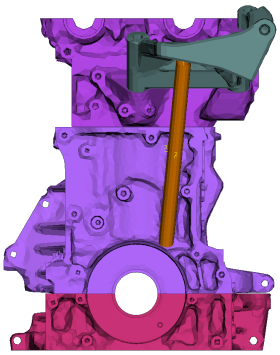

(f) Suspension point support. The RHM stiffened from the block. Bar attachment located far from the cylinder head, near the suspension point of the RHM.

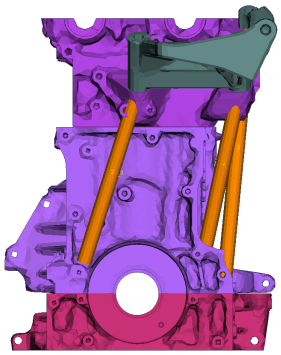

(g) Left & right block hinged support. The hinged RHM stiffened from the engine block, with support from both right and left part. Note the differences in bar attachment to the RHM compared to (a).

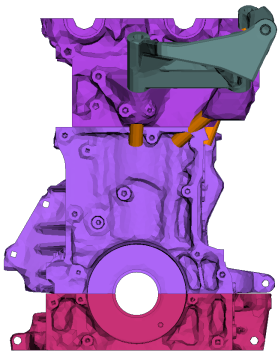

(h) Block top hinged support. The hinged RHM stiffened from the top of the engine block. Note the differences in bar attachment to the RHM compared to (c).

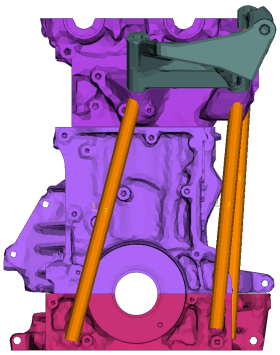

(i) Bed plate hinged support. The hinged RHM stiffened from the bed plate. Note the differences in bar attachment to the RHM compared to (d).

Figure 4.2: The nine different modelled RHM consoles. (a), (b), (c), (d), (e) and (f) are the generally stiffened consoles and (g), (h) and (i) are the hinged consoles.

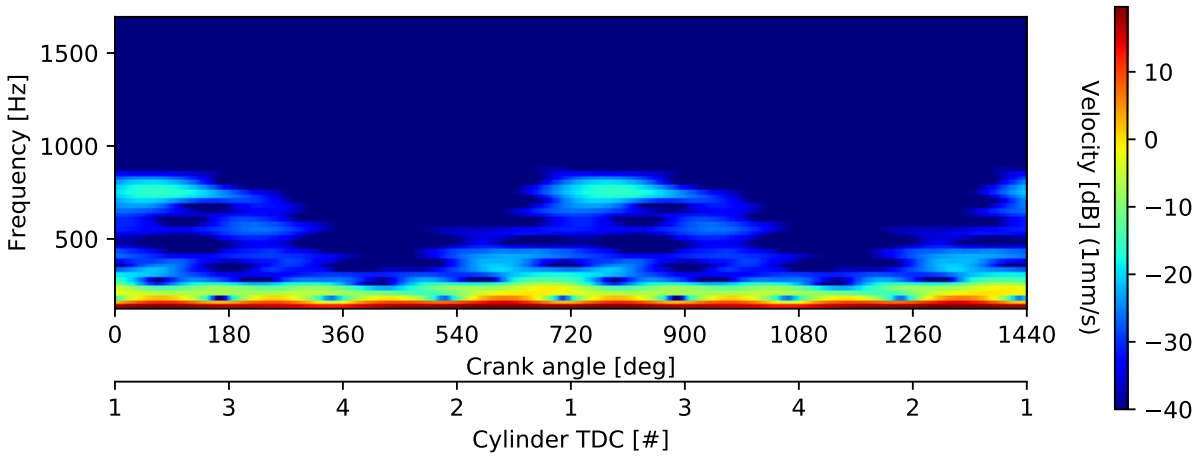

Figure 4.3: Spectrogram of vertical velocity at the RHM, simulated during two engine cycles. Engine speed 1500 rpm. Left & right block support configuration. The time instances for cylinder TDC are outlined at the bottom.

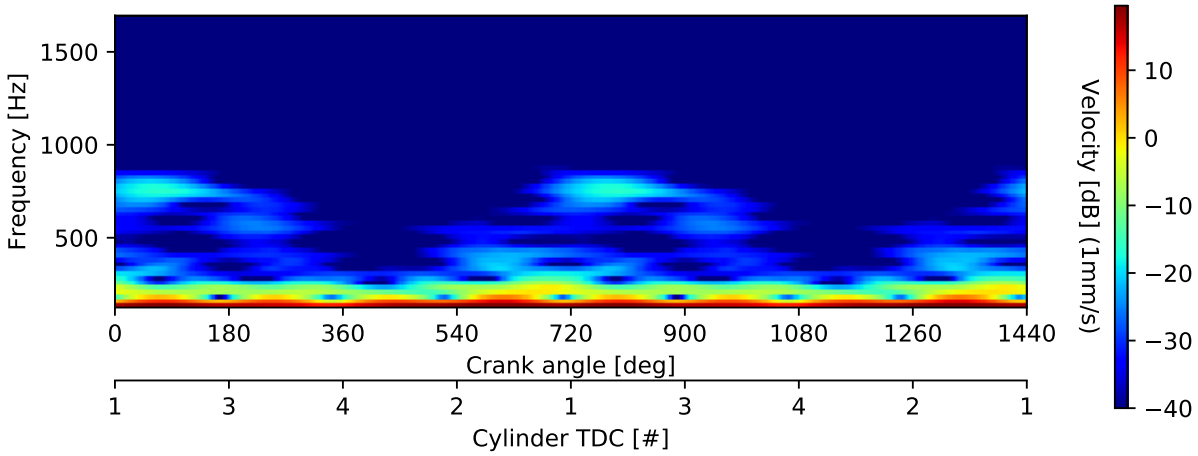

Figure 4.4: Spectrogram of vertical velocity at the RHM, simulated during two engine cycles. Engine speed 1500 rpm. Right block support configuration. The time instances for cylinder TDC are outlined at the bottom.

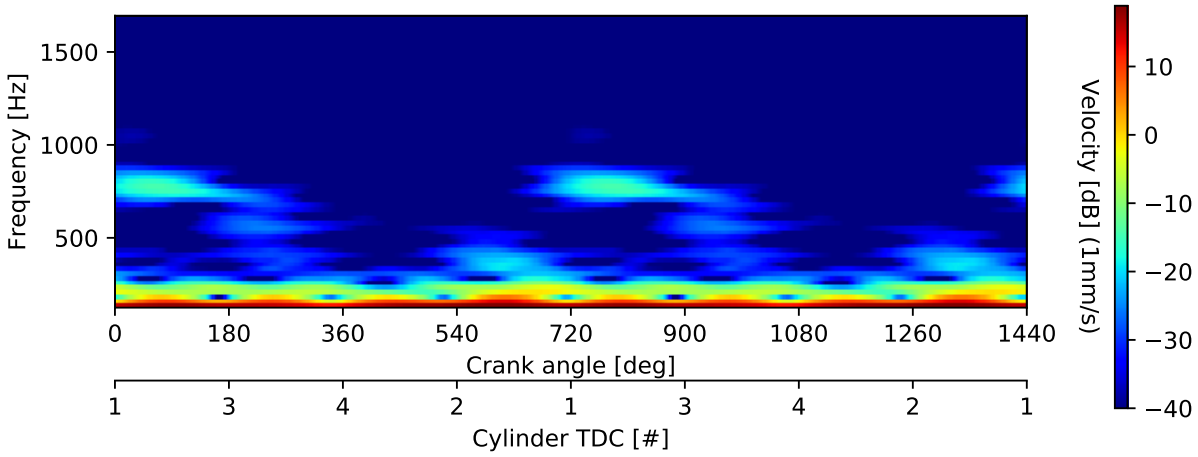

Figure 4.5: Spectrogram of vertical velocity at the RHM, simulated during two engine cycles. Engine speed 1500 rpm. Block top support configuration. The time instances for cylinder TDC are outlined at the bottom.

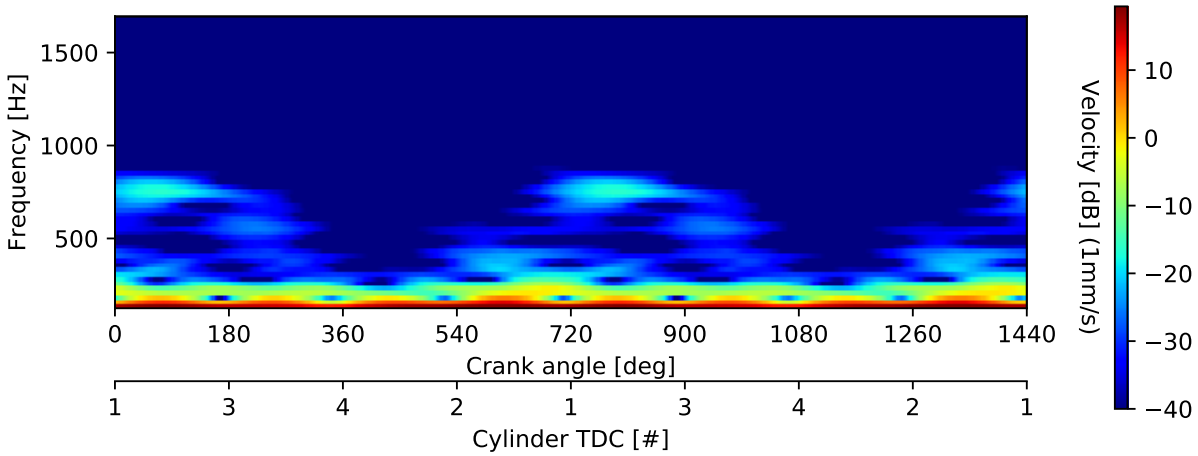

Figure 4.6: Spectrogram of vertical velocity at the RHM, simulated during two engine cycles. Engine speed 1500 rpm. Bed plate support configuration. The time instances for cylinder TDC are outlined at the bottom.

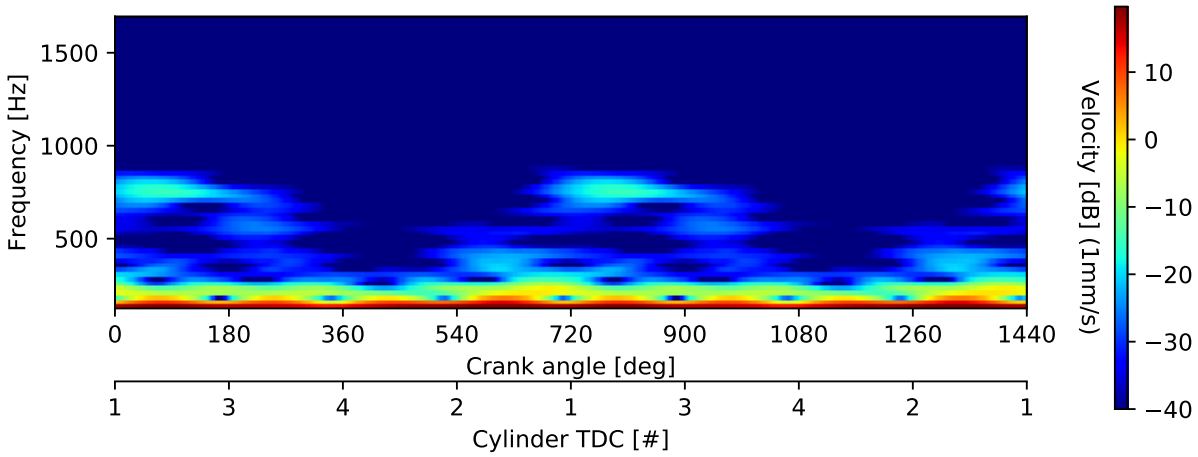

Figure 4.7: Spectrogram of vertical velocity at the RHM, simulated during two engine cycles. Engine speed 1500 rpm. Cylinder head support configuration. The time instances for cylinder TDC are outlined at the bottom.

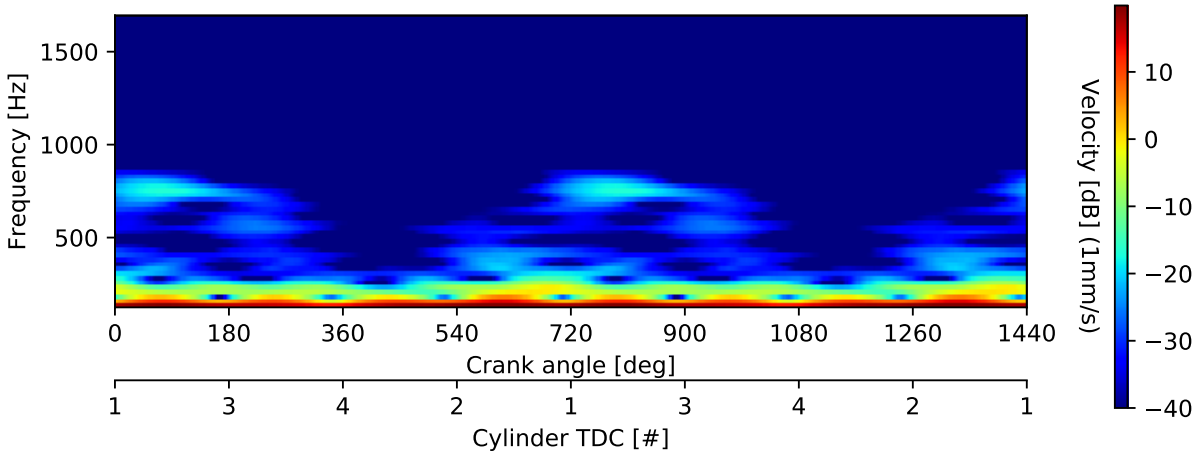

Figure 4.8: Spectrogram of vertical velocity at the RHM, simulated during two engine cycles. Engine speed 1500 rpm. Suspension point support configuration. The time instances for cylinder TDC are outlined at the bottom.

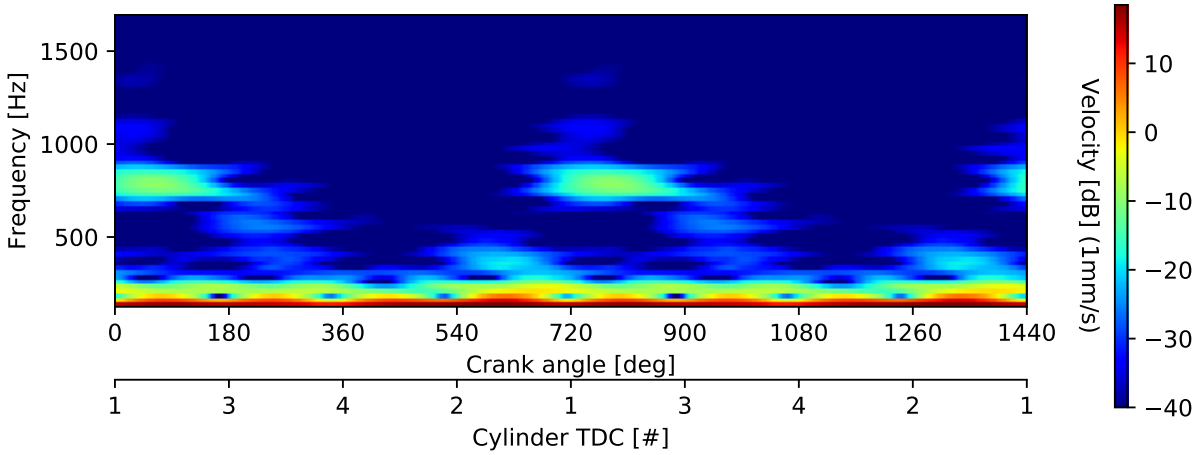

Figure 4.9: Spectrogram of vertical velocity at the RHM, simulated during two engine cycles. Engine speed 1500 rpm. Left & right block hinged support configuration. The time instances for cylinder TDC are outlined at the bottom.

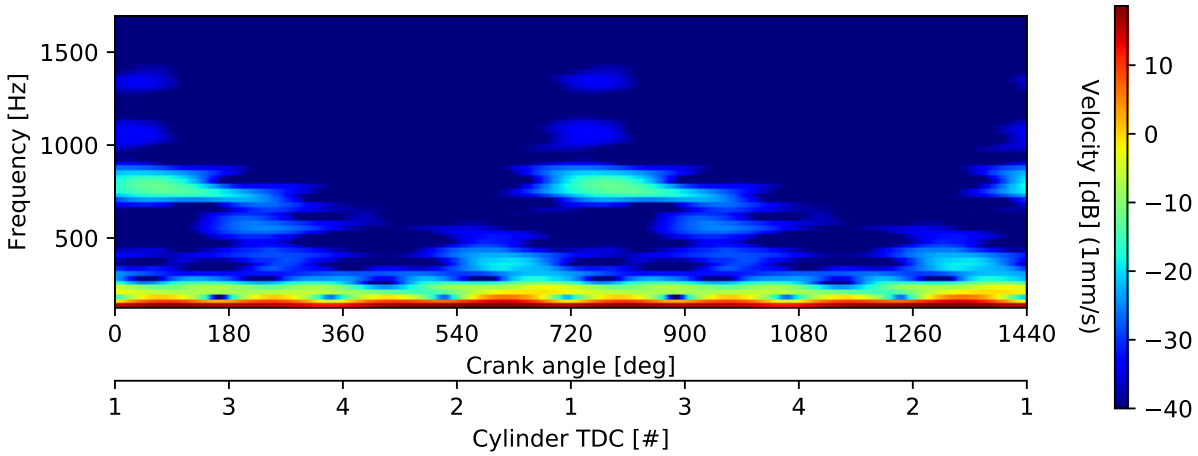

Figure 4.10: Spectrogram of vertical velocity at the RHM, simulated during two engine cycles. Engine speed 1500 rpm. Block top hinged support configuration. The time instances for cylinder TDC are outlined at the bottom.

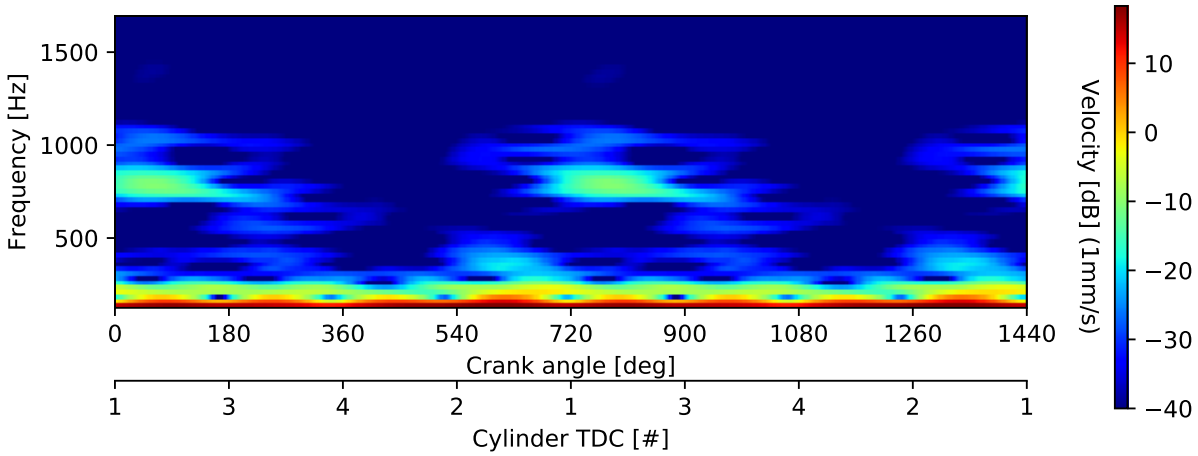

Figure 4.11: Spectrogram of vertical velocity at the RHM, simulated during two engine cycles. Engine speed 1500 rpm. Bed plate hinged support configuration. The time instances for cylinder TDC are outlined at the bottom.

5 Discussion

The impulsive noise character perceived in the vehicle cabin is a vast subject and the psychoacoustic nature makes it intricate to evaluate. Furthermore the internal combustion engine is in itself difficult to model and the combination makes for a scope of immense proportions. The need for limitations is therefore crucial.

The current study accounts only for a single engine type. However, the results are believed to be reasonably universal and applicable to similar engines using the same spark ignition technique. The assumption is supported by the fact that the results from this project and the results from [2] correlate fairly well.

The applied numerical model of the engine has been extensively used at Volvo Cars. According to the provider of the model it is believed to accurately capture modal behaviour up to approximately 500 Hz. However, the trends and overall appearances at higher frequencies are regarded reliable when compared to the baseline case, acting as a reference. The absolute magnitude and frequency should not be regarded as true, however the relative magnitude and frequency differences should. The need for model evaluation and development is regarded as unnecessary, unless the capture of correct absolute magnitudes of higher frequency modes are required, as the primary purpose of the model is qualitative assessments. To reduce the simulation time in the current project two changes were made to the model; (1) gears within the gearbox were omitted and (2) the braking torque was applied directly at the torque converter. The simplified model captures the same behaviour as the full model and is regarded satisfactory.

The evaluation of impulsiveness is the essence of the project. Due to its psychoacoustic nature it is hard to quantify, however the PAPR of velocity and acceleration is believed to be a promising estimate. During the project it became apparent that the PAPR can not be used exclusively as a way to estimate the impulsiveness, as information about frequency content and vibration magnitude might be lost and, as a consequence, the results interpreted in a misleading way. However, the PAPR is a suitable metric to estimate the impulsiveness whilst also incorporating a way of considering masking effects. By combining PAPR with spectrograms the analysis of different cases is more profound, and not only is it possible to evaluate if impulsiveness is to be expected but also at what frequencies and due to what impulse event in the engine (typically combustion in a cylinder) the impulsiveness occurs. The coarse scale of the spectrograms may lack resolution to study impulsive regions in detail, but were chosen deliberately to give an overall understanding of the spectrogram. The interpretation of the results from such a detailed study is not straightforward. For instance, without knowing if e.g. the peak value of the impulsive region or the gradient of the same is what is affecting the perceived impulsiveness, information would be useless. Hence, the scale was selected coarse and it is left as a recommendation to further investigate how to more thoroughly interpret the spectrograms.

The identification of cylinder number 1 as the main excitation source of the impulsive noise character and the RHM as the main transfer path has been enabled by the combination of evaluation methods. The reduction of impulsive noise character may not necessarily guarantee a *better* sounding engine and the addition of the estimated average sound pressure levels may not only aid to correctly evaluate the PAPR data but also give some basic insight into the general noise levels. The informal listening has further aided the evaluation and provided useful insight in conjunction with the other evaluation methods. Although the reduction of impulsive noise character was the goal for this project, a rather important contribution of the work is that it has enabled and may further enable a more elaborate assessment of different engines.

The screening of potential countermeasures for impulsive noise character is possibly the most important contribution of the project, yielding results about several potential countermeasures. The selection of parameters includes structural properties such as mass- and stiffness, as well as combustion strategies and bearing clearances. Damping properties have not been considered, and it may be valuable to also study how those types of alterations affect the model outcome before deciding on alterations to implement. Using the OFAT design enabled a straightforward process as well as easily interpretable results. According to the literature it is a suitable procedure to estimate the importance of selected parameters, with respect to a target variable, and it did enable the selection of interesting parameters to investigate further. Variance based methods are also suggested in literature, but were rejected for the current investigation due to their more computational expensive nature. The selection of an evaluation quantity is not obvious, and is still regarded as a non resolved matter. The principal behaviour of the pronounced pulse is present regardless of whether the velocity or acceleration is studied, however the two quantities do not always show the same trend or magnitude of change for the same

parameter alteration and it may be unreliable to only account for one without further investigation. The screening resulted in valuable insight in how engine modifications affect the impulsiveness.

The identification and selection of important mounting points have been aided further by the EEM. The RHM has been concluded to be the most important mounting point to consider when analysing the impulsive noise character. The EEM further enabled a more detailed insight in how the, for the detailed parameter analysis, four selected parameters may suppress the impulsiveness and its respective relevance of implementation. The hypothesis that the mass-stiffness ratio between the cylinder head and engine mount, and base structure and engine mount, respectively, causes the impulsive noise character when the engine is exposed to impulses could be concluded as too simple to explain the complex phenomenon of the impulsive noise character. This result is further emphasised by comparing the three different retardation alterations from the parameter screening. It appears as if the impulse from cylinder number 1 is cancelled by one or several of the other cylinders. Typically a retarded spark event is regarded not desirable from an emission and performance perspective, however yields a less sharp pressure pulse and is thus of interest for this project. If the impulse from cylinder number 1 is cancelled by one or several of the other cylinders, potentially it could be beneficial to have an even harsher combustion strategy for the cylinder(s) identified as the cancelling ones, and have the engine as a hole to operate at the same or better emission and performance levels as today.

The mass- and stiffness alterations of the RHM did not yield any substantial improvements, with respect to impulsiveness. The resulting spectrograms are seemingly identical to those of the baseline indicating that the vibrations transmitted from the engine to the car is not affected by the modal behaviour of the RHM to a significant extent. It could be argued that the modal behaviour of the transfer path should matter more, however the confidence in the evaluation methods are high and the results regarded as valid. The informal listening disagrees, but the accuracy of the combined results from the PAPR data and the spectrograms are together believed to be more reliable than the slight differences heard in the informal listening. Although the mass- and stiffness alteration had a moderate effect on impulsiveness, the redesign of the same appears to be a promising countermeasure. The PAPR of velocity and acceleration suggest a significant improvement for nearly any type of redesign. However, when including the spectrograms in the analysis there are ambiguities between the two evaluation methods. It may be difficult to fully understand what type of change a redesigned RHM would mean for the sound characteristics in the vehicle cabin, it is however safe to say that a redesign of the RHM would be beneficial and a highly important part to look further in to.

Even though a combination of assessments for the impulsive noise character have been used it is still not straightforward, if at all possible, to reliably quantify how good or bad an engine configuration is. Unless large differences exist a qualitative assessment may also be unreliable. Some evaluated cases yield easily interpretable data where conclusions may be drawn with high confidence. Some other cases do not, and for these more or less accurate predictions may be done. Cases in the second category may require further study if they are found interesting. The subjective nature of the noise phenomenon dismisses the use of physical evaluation metrics and the subjectiveness of the human hearing have to be considered.

6 Conclusions

The difficulty to evaluate impulsive noise character has been discussed in this report. However, the combination of proposed evaluation methods have revealed valuable insight and enabled important conclusion to be drawn.

It may, with confidence, be stated that there exist countermeasures to the impulsive noise character. These have been identified using evaluation methods (PAPR of velocity and acceleration, spectrograms of velocity and informal listening) that are concluded to be satisfactory when used in conjunction with an overall estimate of sound pressure levels, and more importantly each other. Together these capture the basics of the relevant psycoacoustic concepts needed to be considered.

The ignition event in cylinder number 1 is found to be the main excitation source for the impulsiveness, although with interactions from the other cylinders, and the working hypothesis of the RHM as the main transfer path of vibrations between the engine and the car is validated. It may also be stated that the modal behaviour of the RHM seems to be irrelevant regarding the structure borne noise characteristics.

The list below summarises the relevant conclusions from the project. Further down the recommended countermeasures are presented.

- The impulsive noise character is a complex sound phenomenon. It is difficult to quantify and measure, and qualitative assessments may also fail.
- The impulsive noise character may be perceived favourable or disfavourable, depending on driving scenario.
- Countermeasures to the impulsive noise character exist.
- The ignition event in cylinder number 1 is the main excitation source to the impulsive noise character.
- The impulse from cylinder number 1 can potentially be cancelled by the other cylinders and it could indicate that it would be beneficial to have a less harsh combustion in cylinder number 1 and a more harsh combustion in the identified cancelling cylinders. A combustion strategy like that would not only reduce the impulsive noise character, but also have less of an impact on emissions and performance than more drastic combustion strategies. This conclusion requires further investigation to be conclusive.
- The RHM is the main transfer path of the impulsive noise character.
- The modal behaviour of the RHM does only have a moderate influence on the structure borne noise characteristics.
- PAPR is a suitable estimate for impulsiveness, however not complete without the use of spectrograms and overall sound pressure levels.
- The assessed physical quantity have to be selected with care.
- The hypothesis about the mass-stiffness ratio between the cylinder head and engine mount, and base structure and engine mount, respectively, may be too simple to fully explain the impulsive noise character.
- Several parameters have been found to have a negligible influence on the impulsive noise character:
    1. The cylinder head (mass and stiffness)
    2. The RHM (mass and stiffness)
    3. The main bearing clearance
- Several parameters have been found to have a significant influence on the impulsive noise character:
    1. The block & bed plate side (mass and stiffness)
    2. The crank shaft stiffness (general and shank)
    3. Cylinder retardation
    4. Combustion duration
    5. Redesign of the RHM

Proposed countermeasures

To suppress the structure borne impulsive noise character of the internal combustion engine, perceived in the vehicle cabin, the following three efficient countermeasures are suggested and recommended.

1. **Stiffen the crank shaft. If not possible to increase main bearing diameter, by only stiffening the shanks a significant improvement would be achieved.**

2. **Extend the combustion duration by phasing the camshafts. Even a small change in duration results in relatively large impulsive noise character reduction.**

3. **Redesign the RHM to (also) take support from further down on the engine block or bed plate. A mere connection would suffice to yield considerable results. Strive for giving support on the RHM near the mounting point with the car to further increase the effect.**

7 Recommendations for future work

Countermeasures as well as irrelevant mitigation actions for impulsive noise character in vehicle compartments have been identified by this project. This includes the investigation of root causes, noise generation explanations and primary transfer paths. However, the study of the impulsive noise character phenomenon and its related subjects is vast, and a complete and comprehensive study of the field does not fit in a single master's thesis report. To comprehensively understand and with precision predict the impulsive noise character future work is needed.

Recommendations for future work may be divided into three primary subcategories; (1) assessment criteria for evaluation of the impulsiveness perceived by the human hearing, (2) understanding the root causes that give rise to the impulsive noise character and (3) modelling and methods to investigate the phenomenon.

7.1 Assessment criteria for evaluation of impulsiveness

The field of psychoacoustics is in itself very extensive. Although mainly loudness predictions and annoyance estimates are required, this still makes for a large scope. In the report it is argued that the PAPR constitutes a credible estimate for impulsiveness but also that it does not fully illuminate all aspects of the noise characteristics. It was used in conjunction with velocity spectrograms in order to capture frequency variations in combustion related time scales and aided by overall sound pressure level estimates. To further validate the conclusions subjective listening was used. All these methods are deemed necessary to reliably assess the impulsive noise character. However, the process is somewhat cumbersome and not fully satisfactory.

The selection of an evaluation quantity is not obvious. The chosen quantity may have a large impact on the results and the drawn conclusions may depend on the selection of the quantity. Although the combination of acceleration and velocity used in this project is believed to have enabled conclusions that capture the general behaviour of the engine, it is recommended to evaluate why the quantities differ as they do and to, if possible, propose the selection of the one that best captures the impulsive noise character.

In literature attempts have been made to quantify impulsiveness by a single metric, more elaborate than the PAPR. In [1] it was stated that the pulse width was important for the loudness perception. For a future study it is recommended to evaluate the possibility to incorporate such a metric, where it is proposed to start with an extended PAPR evaluation where not only the peak value but also the pulse width is taken into account. A new evaluation factor F is created and named the attenuated loudness estimate expectation (ALEX) and defined according to Equation (7.1) below.

$$F_{\mathrm{ALEX}} \equiv \left(\frac{a_{\mathrm{peak}} a_{\mathrm{width}}}{a_{\mathrm{RMS}}} \right)^2 \tag{7.1}$$

Where a_{width} is defined as the pulse width in units of time or crank shaft angles for when the pulse has a magnitude greater than a_{RMS}.

Another recommendation is to study the spectrograms further, especially the main impulsive region, and to analyse whether now seemingly minor changes may actually have a large impact on the perceived noise. It would further be of interest to understand how much of a difference a change in PAPR or spectrogram makes for the perceived noise. Although already performed at Volvo Cars, since the PAPR is the only present quantitative metric, and in this project not always conclusive with the other evaluation methods, it would be recommended to further investigate the correlation between the PAPR value and subjectively perceived impulsive noise character. In general a better understanding between the evaluation methods and the actually perceived noise characteristics would be beneficial.

In short, the following is recommended to study further:

- The evaluation of impulsiveness. Develop a metric to better capture the impulsive noise character. As a starting point, the ALEX-factor is proposed.

- Investigate the discrepancies between different evaluation quantities and propose the "correct" one to use.
- Examine the spectrograms more thoroughly.
- Investigate the existence of a correlation between PAPR and/or other evaluation methods and perceived noise.

7.2 Root causes

Apart from better understanding the characteristics of the perceived noise it would also be beneficial to better understand the mechanisms from which the impulsive noise character originates. It is confidently stated that the impulses from the combustion events in the cylinders, and most relevant in cylinder number 1, are the main cause for the impulsive noise character. However, the coupling is not direct and a more meticulous investigation with the aim to better understand the root cause is needed to fully comprehend the effect of possible mitigation actions. The working hypothesis that the mass-stiffness ratio between the cylinder head and engine mount, and base structure and engine mount, respectively, is satisfactory but may need to be extended.

During the project structural components have only been investigated by mass- and stiffness alterations. To further understand the origin and possible mitigation actions it is recommended to also investigate how damping properties affect the transferred sound character.

In short, the following is recommended to study further:

- The mechanisms of origin of the impulsive noise character. Extend the current working hypothesis, or if needed construct a new.
- Incorporate damping properties in the study.

7.3 Modelling and methods

The evaluation of the impulsive noise character is dependent on a reliable investigation approach and methodology. Although the implemented way of work is believed to be satisfactory in this project, some future work is recommended.

If in a future project the implemented EEM is of interest it is recommended that the trajectories are selected as subsets of a larger set of trajectories, as discussed in Section 3.4. It would guarantee a better coverage of the parameter range.

The investigation of mounting strategies in the design study revealed that the three hinged support cases had an unexpected modal behaviour. Consequently the validity of these results are questionable, and it is recommended to further study how to properly model the desired console mounting. On a more general matter the impact of a redesigned RHM console is not conclusive based on the available evaluation methods, and further studies have to be performed to reliably conclude effects on the impulsive noise character that the different design cases have.

In short, the following is recommended to study further:

- If performing an EEM study, select trajectories as a subset of a larger number of generated trajectories.
- Investigate the *correct* way to achieve the desired hinged RHM support design cases.
- Investigate and further explore what the actual change in noise characteristics would be, based on a redesigned RHM console.

References

[1] G. M. Ballou. *Handbook For Sound Engineers*. 3rd ed. Focal Press, 2002. ISBN: 0-240-80454-6.

[2] B. Graf, A. Rust, M. Mehrgou, and H. Zhenyue. Effect of Cranktrain Design on Engine NVH Performance. *MTZ worldwide* **78**.9 (Sept. 2017), 70–75. ISSN: 2192-9114. DOI: 10.1007/s38313-017-0087-9. URL: https://doi.org/10.1007/s38313-017-0087-9.

[3] A. Sontacchi, R. Holdrich, J. Girstmair, H. Allmaier, S. Bikker, and A. Rust. Predicted Roughness Perception for Simulated Vehicle Interior Noise. *SAE International Journal of Engines* **5**.3 (June 2012), 1524–1532. ISSN: 1946-3944. DOI: https://doi.org/10.4271/2012-01-1561. URL: https://doi.org/10.4271/2012-01-1561.

[4] W. Song, H. Saito, and K. Haddad. "Improved Noise Source Identification Using Sound Quality Metrics Mapping in Vehicle Noise Measurements". *SAE 2011 Noise and Vibration Conference and Exhibition*. SAE International, May 2011. DOI: https://doi.org/10.4271/2011-01-1671. URL: https://doi.org/10.4271/2011-01-1671.

[5] M. Blommer, A. Eden, and S. Amman. "Sound Quality Metric Development and Application for Impulsive Engine Noise". *SAE 2005 Noise and Vibration Conference and Exhibition*. SAE International, May 2005. DOI: https://doi.org/10.4271/2005-01-2482. URL: https://doi.org/10.4271/2005-01-2482.

[6] M. A. A. A. Blommer. "Automated psychoacoustic based method for detecting borderline spark knock". U.S. Patent 6012426. Jan. 11, 2000. URL: http://patft.uspto.gov/netacgi/nph-Parser?Sect1=PTO1&Sect2=HITOFF&d=PALL&p=1&u=%2Fnetahtml%2FPTO%2Fsrchnum.htm&r=1&f=G&l=50&s1=6012426.PN.&OS=PN/6012426&RS=PN/6012426 (visited on 10/12/2018).

[7] S. Amman, M. Blommer, and J. Greenberg. An auditory model for the prediction of detection thresholds of impulsive sound events. **108** (Nov. 2000).

[8] H. Tienhaara. Guidelines to engine dynamics and vibration (2004).

[9] URL: https://www.ansa-usa.com/software/ansa/.

[10] URL: http://www.mscsoftware.com/product/msc-nastran.

[11] URL: https://www.ansa-usa.com/software/meta/.

[12] URL: https://www.avl.com/excite.

[13] J. O. Smith. *Spectral Audio Signal Processing*. online book, 2011 edition. URL: http://ccrma.stanford.edu/~jos/sasp/ (visited on 01/24/2019).

[14] A. Saltelli, K. Chan, and E. M. Scott. *Sensitivity Analysis*. John WIley & Sons Ltd, 2000. ISBN: 0-471-99892-3.

[15] H. M. Wainwright, S. Finsterle, Y. Jung, Q. Zhou, and J. T. Birkholzer. Making sense of global sensitivity analyses. *Computers & Geosciences* **65** (2014). TOUGH Symposium 2012, 84–94. ISSN: 0098-3004. DOI: https://doi.org/10.1016/j.cageo.2013.06.006. URL: http://www.sciencedirect.com/science/article/pii/S0098300413001702.

[16] M. D. Morris. Factorial Sampling Plans for Preliminary Computational Experiments. *Technometrics* **33**.2 (May 1991), 161–174.

[17] F. Campolongo, J. Cariboni, and A. Saltelli. An effective screening design for sensitivity analysis of large models. *Environmental Modelling & Software* **22**.10 (2007). Modelling, computer-assisted simulations, and mapping of dangerous phenomena for hazard assessment, 1509–1518. ISSN: 1364-8152. DOI: https://doi.org/10.1016/j.envsoft.2006.10.004. URL: http://www.sciencedirect.com/science/article/pii/S1364815206002805.

[18] J. P. Norton. Selection of Morris Trajectories for Initial Sensitivity Analysis. *IFAC Proceedings Volumes* **42**.10 (2009). 15th IFAC Symposium on System Identification, 670–674. ISSN: 1474-6670. DOI: https://doi.org/10.3182/20090706-3-FR-2004.00111. URL: http://www.sciencedirect.com/science/article/pii/S1474667016387250.

[19] H. C. van Houwelingen, H. C. Boshuizen, and M. Capannesi. Sensitivity analysis of state-transition models: How to deal with a large number of inputs. *Computers in Biology and Medicine* **41**.9 (2011), 838–842. ISSN: 0010-4825. DOI: https://doi.org/10.1016/j.compbiomed.2011.07.001. URL: http://www.sciencedirect.com/science/article/pii/S0010482511001429.

A Elementary effects method sampling generation

Below the sampling generation procedure for the ten trajectories is presented.

```
%--------------------------------------------------------------------------
%
%       Author: Alexander Olsson
%
%       Description: A simple code that normalises and (pseudo)randomly
%       creates a numTrajectories amount of simulation trajectories
%       according to the Elementary Effects Method (Morris), with
%       numPartition number of parameter interval partitioning.
%
%       Each row in each Bstar-matrix corresponds to a (normalised)
%       simulation set-up.
%
%--------------------------------------------------------------------------

clc
clear variables
close all

%% User defined inputs
numTrajectories = 10; %r, number of trajectories
numPartition = 4; %p, number of partitions

%       Block   Crank   Cyl. head   L. duration
xMin = [75      210     75          1];     % Minimum parameter values
xMax = [150     420     150         4];    % Maximum parameter values

numVariables = length(xMin); %k, number of variables


%% Main loop
for q = 1:numTrajectories
    %% xStar
    unitInterval = zeros(numVariables,numPartition); %normalised distribution, [0,1]
    xStar = zeros(numVariables,numPartition); % random base values

    for i = 1:numVariables
        for j = 1:numPartition
            xStar(i,j) = datasample(linspace(xMin(i), xMax(i), numPartition),1);
            xStar(i,j) = (xStar(i,j)-xMin(i))/(xMax(i)-xMin(i));
        end
        unitInterval(i,:) = linspace(xMin(i), xMax(i), numPartition);
        unitInterval(i,:) = (unitInterval(i,:)-xMin(i))/(xMax(i)-xMin(i));
    end
    xStar = xStar(:,randi([1 length(xStar(1,:))]))'; % select a random set

    %% B
    B = ones(numVariables+1,numVariables);
    k=1;
    for i = 1:numVariables+1
        B(i,k:end)=0;
        k=k+1;
    end


    %% Dstar
    Dstar = zeros(numVariables);
    r = randi([1 2],4,1);
    for i = 1:numVariables
        if r(i) == 2
            r(i) = -1;
        else
```

```
        end
        Dstar(i,i) = r(i);
    end


    %% Jmk
    Jmk = ones(numVariables+1, numVariables);


    %% Pstar
    Pstar = zeros(numVariables, numVariables);
    r = randperm(numVariables);
    for i = 1:length(Pstar)
        Pstar(i,r(i)) = 1;
    end


    %% Delta
    delta = numPartition/(2*(numPartition-1));


    %% Bstar
    BstarOriginal{q} = (Jmk(:,1)*xStar+0.5*delta*((2*B-Jmk)*Dstar+Jmk))*Pstar;
    Bstar{q} = BstarOriginal{q};

    % If the addition of delta goes out of the parameter range, subtract
    % delta instead (i.e. subtract the added delta and then delta again)
    for i = 1:numVariables+1
        for j = 1:numVariables
            if Bstar{q}(i,j) > 1
                Bstar{q}(i,j) = BstarOriginal{q}(i,j)-2*delta;
            else
            end
            BstarReal{q}(i,j) = Bstar{q}(i,j).*(xMax(j)-xMin(j))+xMin(j);
        end
    end

    %% Printing and saving
    disp(BstarOriginal{q})
    disp(Bstar{q})
    disp(BstarReal{q})
    dlmwrite('BstarOriginal.txt',BstarOriginal{q},'-append','delimiter','\t','precision',3)
    dlmwrite('Bstar.txt',Bstar{q},'-append','delimiter','\t','precision',3)
    dlmwrite('BstarReal.txt',BstarReal{q},'-append','delimiter','\t','precision',3)
end
```

B Elementary effects method sampling matrices

In Table B.1 below the ten trajectory matrices for the EEM are shown, for both normalised- and real values. The block & bed plate side stiffness is called "B", the crank shaft stiffness is called "CR", the cylinder head stiffness is called "CH" and the combustion duration is called "D" in the table.

Table B.1: The EEM sampling matrices.

EEM Matrices							
Normalised				Real			
B	CR	CH	D	B [GPa]	CR [GPa]	CH [GPa]	D [deg]
B1							
2/3	1/3	2/3	2/3	125	280	125	34
2/3	1/3	0	2/3	125	280	75	34
0	1/3	0	2/3	75	280	75	34
0	1	0	2/3	75	420	75	34
0	1	0	0	75	420	75	28
B2							
0	0	1	0	75	210	150	28
0	0	1/3	0	75	210	100	28
2/3	0	1/3	0	125	210	100	28
2/3	0	1/3	2/3	125	210	100	34
2/3	2/3	1/3	2/3	125	350	100	34
B3							
0	1/3	2/3	1/3	75	280	125	31
0	1	2/3	1/3	75	420	125	31
0	1	2/3	1	75	420	125	36
2/3	1	2/3	1	125	420	125	36
2/3	1	0	1	125	420	75	36
B4							
1	1	1	0	150	420	150	28
1	1	1/3	0	150	420	100	28
1/3	1	1/3	0	100	420	100	28
1/3	1	1/3	2/3	100	420	100	34
1/3	1/3	1/3	2/3	100	280	100	34
B5							
1/3	1	1/3	2/3	100	420	100	34
1	1	1/3	2/3	150	420	100	34
1	1	1	2/3	150	420	150	34
1	1/3	1	2/3	150	280	150	34
1	1/3	1	0	150	280	150	28
B6							

Table B.1 continued from previous page

EEM Matrices							
1	0	1/3	0	150	210	100	28
1	0	1	0	150	210	150	28
1	2/3	1	0	150	350	150	28
1	2/3	1	2/3	150	350	150	34
1/3	2/3	1	2/3	100	350	150	34
B7							
0	1/3	2/3	0	75	280	125	28
2/3	1/3	2/3	0	125	280	125	28
2/3	1/3	2/3	2/3	125	280	125	34
2/3	1	2/3	2/3	125	420	125	34
2/3	1	0	2/3	125	420	75	34
B8							
2/3	0	1	0	125	210	150	28
2/3	2/3	1	0	125	350	150	28
2/3	2/3	1	2/3	125	350	150	34
2/3	2/3	1/3	2/3	125	350	100	34
0	2/3	1/3	2/3	75	350	100	34
B9							
0	2/3	2/3	1	75	350	125	36
0	2/3	2/3	1/3	75	350	125	31
0	0	2/3	1/3	75	210	125	31
2/3	0	2/3	1/3	125	210	125	31
2/3	0	0	1/3	125	210	75	31
B10							
1	0	2/3	1/3	150	210	125	31
1	0	0	1/3	150	210	75	31
1	2/3	0	1/3	150	350	75	31
1	2/3	0	1	150	350	75	36
1/3	2/3	0	1	100	350	75	36

C Parameter screening PAPR data

In Tables C.1, C.2, C.3, C.4, C.5, C.6, C.7, C.8, C.9 and C.10 the velocity and the acceleration PAPR data for the parameter screening, combined with each DOFs sensitivity metric, for the RHM, the LHM, the RUTB, the RLTB and the LLTB, respectively, are presented.

Structural parameter alterations are compared to the baseline when performing the sensitivity analysis, whereas the combustion strategy alterations are compared to the baseline with pressure data for only one engine speed. That case is called *STD*.

The comparison of the absolute PAPR values for the different mounting points has lead to the selection of the RHM and RLTB in the vertical direction as the most relevant and important to study.

C.1 RHM

Table C.1: All calculated PAPR data for the velocity in the RHM with corresponding SA metrics for all DOFs for the parameter screening.

Velocity (RHM)						
	DOF1	**LSA1**	**DOF2**	**LSA2**	**DOF3**	**LSA3**
Baseline	17.6		15.1		23.8	
Block & bed plate side mass	16.4	0.068	13.3	0.119	17.9	0.248
Block & bed plate side stiffness	16.4	0.068	13.3	0.119	17.9	0.248
Crank shaft general stiffness	20.2	-0.148	21.7	-0.437	19.6	0.176
Crank shaft shank stiffness	22.1	-0.256	18.3	-0.212	21.5	0.097
Cylinder head mass	24.5	-0.392	14.5	0.040	24.4	-0.025
Cylinder head stiffness	18.5	-0.051	17.0	-0.126	22.2	0.067
Main bearing clearance	16.9	0.040	15.6	-0.033	22.6	0.050
RHM mass	21.5	-0.222	13.8	0.086	24.5	-0.029
RHM stiffness	24.0	-0.364	13.7	0.093	24.7	-0.038
STD	12.8		14.5		18.2	
Cylinder no. 1 retardation	11.4	0.109	12.2	0.159	14.6	0.198
Cylinder no. 1-4 retardation	11.6	0.094	13.0	0.103	15.4	0.154
Cylinder no. 4 retardation	13.0	-0.016	14.7	-0.014	18.6	-0.022
Combustion duration						
Long	10.5	0.180	11.5	0.207	8.4	0.538
Short	19.2	-0.500	16.3	-0.124	27.4	-0.505

Table C.2: All calculated PAPR data for the acceleration in the RHM with corresponding SA metrics for all DOFs for the parameter screening.

Acceleration (RHM)						
	DOF1	**LSA1**	**DOF2**	**LSA2**	**DOF3**	**LSA3**
Baseline	30.8		18.6		43.8	
Block & bed plate side mass	25.9	0.159	13.0	0.301	42.7	0.025
Block & bed plate side stiffness	27.1	0.120	13.0	0.301	42.7	0.025
Crank shaft general stiffness	27.2	0.117	22.3	-0.199	35.7	0.185
Crank shaft shank stiffness	33.2	-0.078	21.8	-0.172	41.6	0.050
Cylinder head mass	29.7	0.036	20.9	-0.124	45.3	-0.034
Cylinder head stiffness	26.5	0.140	20.9	-0.124	42.4	0.032
Main bearing clearance	29.3	0.049	19.2	-0.032	40.9	0.066
RHM mass	29.1	0.055	22.2	-0.194	43.9	-0.002
RHM stiffness	30.7	0.003	22.8	-0.226	42.3	0.034
STD	22.3		20.0		32.5	
Cylinder no. 1 retardation	17.1	0.233	17.7	0.115	29.1	0.105
Cylinder no. 1-4 retardation	17.1	0.233	18.8	0.060	32.2	0.009
Cylinder no.4 retardation	24.9	-0.117	20.8	-0.040	34.0	-0.046
Combustion duration						
Long	16.9	0.242	11.2	0.440	22.0	0.323
Short	34.9	-0.565	22.7	-0.135	42.9	-0.320

C.2 LHM

Table C.3: All calculated PAPR data for the velocity in the LHM with corresponding SA metrics for all DOFs for the parameter screening.

Velocity (LHM)						
	DOF1	**LSA1**	**DOF2**	**LSA2**	**DOF3**	**LSA3**
Baseline	13.1		9.4		10.9	
Block & bed plate side mass	12.0	0.084	9.7	-0.032	10.8	0.009
Block & bed plate side stiffness	12.0	0.084	9.7	-0.032	10.8	0.009
Crank shaft general stiffness	11.2	0.145	11.5	-0.223	10.9	0.000
Crank shaft shank stiffness	11.1	0.153	8.4	0.106	11.1	-0.018
Cylinder head mass	13.9	-0.061	8.8	0.064	11.5	-0.055
Cylinder head stiffness	15.6	-0.191	9.3	0.011	11.2	-0.028
Main bearing clearance	14.3	-0.092	9.1	0.032	9.2	0.156
RHM mass	12.8	0.023	9.2	0.021	11.0	-0.009
RHM stiffness	13.0	0.008	9.4	0.000	10.9	0.000
STD	11.6		9.9		11.5	
Cylinder no. 1 retardation	12.1	-0.043	9.9	0.000	11.2	0.026
Cylinder no. 1-4 retardation	11.2	0.034	10.4	-0.051	12.7	-0.104
Cylinder no. 4 retardation	9.5	0.181	9.7	0.020	11.9	-0.035
Combustion duration						
Long	9.2	0.207	9.7	0.020	12.2	-0.061
Short	16.8	-0.448	10.6	-0.071	13.2	-0.148

Table C.4: All calculated PAPR data for the acceleration in the LHM with corresponding SA metrics for all DOFs for the parameter screening.

Acceleration (LHM)						
	DOF1	**LSA1**	**DOF2**	**LSA2**	**DOF3**	**LSA3**
Baseline	20.8		11.1		19.5	
Block & bed plate side mass	19.3	0.072	11.7	-0.054	18.8	0.036
Block & bed plate side stiffness	19.3	0.072	11.7	-0.054	19.0	0.026
Crank shaft general stiffness	24.6	-0.183	11.9	-0.072	14.7	0.246
Crank shaft shank stiffness	16.9	0.188	13.0	-0.171	17.5	0.103
Cylinder head mass	20.7	0.005	11.4	-0.027	20.2	-0.036
Cylinder head stiffness	22.3	-0.072	10.5	0.054	19.7	-0.010
Main bearing clearance	20.0	0.038	12.3	-0.108	18.9	0.031
RHM mass	20.4	0.019	11.1	0.000	19.3	0.010
RHM stiffness	20.5	0.014	11.1	0.000	19.5	0.000
STD	17.9		11.7		20.3	
Cylinder no. 1 retardation	19.0	-0.061	12.8	-0.094	21.1	-0.039
Cylinder no. 1-4 retardation	17.3	0.034	11.7	0.000	18.9	0.069
Cylinder no. 4 retardation	15.5	0.134	11.5	0.017	17.3	0.148
Combustion duration						
Long	13.9	0.223	12.6	-0.077	12.9	0.365
Short	27.9	-0.559	15.9	-0.359	27.3	-0.345

C.3 RUTB

Table C.5: All calculated PAPR data for the velocity in the RUTB with corresponding SA metrics for all DOFs for the parameter screening.

Velocity (RUTB)						
	DOF1	**LSA1**	**DOF2**	**LSA2**	**DOF3**	**LSA3**
Baseline	11.6		9.1		8.5	
Block & bed plate side mass	13.5	-0.164	8.6	0.055	8.3	0.024
Block & bed plate side stiffness	13.5	-0.164	8.6	0.055	8.3	0.024
Crank shaft general stiffness	10.2	0.121	12.2	-0.341	9.2	-0.082
Crank shaft shank stiffness	10.9	0.060	12.1	-0.330	9.3	-0.094
Cylinder head mass	13.0	-0.121	9.5	-0.044	7.9	0.071
Cylinder head stiffness	12.2	-0.052	9.6	-0.055	7.5	0.118
Main bearing clearance	12.0	-0.034	8.3	0.088	8.4	0.012
RHM mass	11.4	0.017	9.1	0.000	7.8	0.082
RHM stiffness	11.6	0.000	8.9	0.022	7.7	0.094
STD	12.0		9.6		7.5	
Cylinder no. 1 retardation	14.0	-0.167	7.6	0.208	8.2	-0.093
Cylinder no. 1-4 retardation	13.4	-0.117	9.5	0.010	7.7	-0.027
Cylinder no. 4 retardation	12.0	0.000	11.0	-0.146	7.6	-0.013
Combustion duration						
Long	11.5	0.042	9.3	0.031	7.1	0.053
Short	13.1	-0.092	9.9	-0.031	7.9	-0.053

Table C.6: All calculated PAPR data for the acceleration in the RUTB with corresponding SA metrics for all DOFs for the parameter screening.

Acceleration (RUTB)						
	DOF1	**LSA1**	**DOF2**	**LSA2**	**DOF3**	**LSA3**
Baseline	17.7		11.4		12.1	
Block & bed plate side mass	16.5	0.068	11.1	0.026	12.5	-0.033
Block & bed plate side stiffness	16.4	0.073	11.1	0.026	12.5	-0.033
Crank shaft general stiffness	22.8	-0.288	9.8	0.140	12.4	-0.025
Crank shaft shank stiffness	18.3	-0.034	7.8	0.316	12.9	-0.066
Cylinder head mass	17.4	0.017	13.6	-0.193	13.3	-0.099
Cylinder head stiffness	17.4	0.017	11.6	-0.018	14.0	-0.157
Main bearing clearance	15.2	0.141	11.7	-0.026	13.6	-0.124
RHM mass	17.4	0.017	14.1	-0.237	11.7	0.033
RHM stiffness	17.3	0.023	14.2	-0.246	11.6	0.041
STD	16.2		9.8		10.7	
Cylinder no. 1 retardation	16.4	-0.012	10.7	-0.092	10.3	0.037
Cylinder no. 1-4 retardation	17.7	-0.093	10.5	-0.071	10.9	-0.019
Cylinder no. 4 retardation	15.9	0.019	10.1	-0.031	10.3	0.037
Combustion duration						
Long	17.5	-0.080	9.1	0.071	9.3	0.131
Short	17.4	-0.074	13.6	-0.388	15.4	-0.439

C.4 RLTB

Table C.7: All calculated PAPR data for the velocity in the RLTB with corresponding SA metrics for all DOFs for the parameter screening.

Velocity (RLTB)						
	DOF1	**LSA1**	**DOF2**	**LSA2**	**DOF3**	**LSA3**
Baseline	8.4		16.8		15.0	
Block & bed plate side mass	8.8	-0.048	13.8	0.179	12.8	0.147
Block & bed plate side stiffness	8.8	-0.048	13.8	0.179	12.9	0.140
Crank shaft general stiffness	6.4	0.238	17.0	-0.012	15.3	-0.020
Crank shaft shank stiffness	6.9	0.179	15.4	0.083	13.7	0.087
Cylinder head mass	8.1	0.036	16.9	-0.006	14.4	0.040
Cylinder head stiffness	7.7	0.083	17.2	-0.024	15.6	-0.040
Main bearing clearance	8.2	0.024	17.8	-0.060	15.4	-0.027
RHM mass	8.3	0.012	16.8	0.000	14.9	0.007
RHM stiffness	8.2	0.024	16.8	0.000	14.9	0.007
STD	8.9		15.6		13.5	
Cylinder no. 1 retardation	8.0	0.101	17.6	-0.128	12.1	0.104
Cylinder no. 1-4 retardation	8.3	0.067	16.1	-0.032	10.5	0.222
Cylinder no.4 retardation	9.1	-0.022	14.8	0.051	14.4	-0.067
Combustion duration						
Long	6.7	0.247	12.7	0.186	8.5	0.370
Short	10.8	-0.213	18.0	-0.154	20.0	-0.481

Table C.8: All calculated PAPR data for the acceleration in the RLTB with corresponding SA metrics for all DOFs for the parameter screening.

Acceleration (RLTB)						
	DOF1	**LSA1**	**DOF2**	**LSA2**	**DOF3**	**LSA3**
Baseline	16.7		24.3		37.0	
Block & bed plate side mass	16.3	0.024	21.9	0.099	32.0	0.135
Block & bed plate side stiffness	16.3	0.024	21.9	0.099	31.9	0.138
Crank shaft general stiffness	20.2	-0.210	21.7	0.107	35.9	0.030
Crank shaft shank stiffness	18.5	-0.108	23.9	0.016	36.6	0.011
Cylinder head mass	16.5	0.012	24.1	0.008	37.6	-0.016
Cylinder head stiffness	15.6	0.066	28.1	-0.156	42.6	-0.151
Main bearing clearance	17.7	-0.060	26.4	-0.086	38.3	-0.035
RHM mass	16.9	-0.012	24.6	-0.012	37.0	0.000
RHM stiffness	16.6	0.006	24.5	-0.008	37.3	-0.008
STD	17.4		23.1		24.7	
Cylinder no. 1 retardation	16.3	0.063	22.8	0.013	24.3	0.016
Cylinder no. 1-4 retardation	17.1	0.017	23.3	-0.009	21.7	0.121
Cylinder no. 4 retardation	18.2	-0.046	23.3	-0.009	24.9	-0.008
Combustion duration						
Long	13.2	0.241	21.6	0.065	21.4	0.134
Short	22.2	-0.276	31.3	-0.355	40.3	-0.632

C.5 LLTB

Table C.9: All calculated PAPR data for the velocity in the LLTB with corresponding SA metrics for all DOFs for the parameter screening.

Velocity (LLTB)						
	DOF1	**LSA1**	**DOF2**	**LSA2**	**DOF3**	**LSA3**
Baseline	15.3		8.0		6.6	
Block & bed plate side mass	14.5	0.052	8.3	-0.038	6.5	0.015
Block & bed plate side stiffness	14.5	0.052	8.3	-0.038	6.6	0.000
Crank shaft general stiffness	7.5	0.510	6.9	0.138	8.0	-0.212
Crank shaft shank stiffness	9.8	0.359	7.1	0.113	6.4	0.030
Cylinder head mass	14.7	0.039	7.7	0.038	6.0	0.091
Cylinder head stiffness	14.8	0.033	8.5	-0.063	6.1	0.076
Main bearing clearance	16.3	-0.065	8.5	-0.063	6.2	0.061
RHM mass	15.3	0.000	8.1	-0.013	6.6	0.000
RHM stiffness	15.3	0.000	8.0	0.000	6.6	0.000
STD	10.1		6.2		5.7	
Cylinder no. 1 retardation	9.3	0.079	7.0	-0.129	6.5	-0.140
Cylinder no. 1-4 retardation	9.5	0.059	6.1	0.016	5.7	0.000
Cylinder no. 4 retardation	9.5	0.059	5.8	0.065	4.9	0.140
Combustion duration						
Long	10.3	-0.020	6.1	0.016	5.3	0.070
Short	10.7	-0.059	6.3	-0.016	6.6	-0.158

Table C.10: All calculated PAPR data for the acceleration in the LLTB with corresponding SA metrics for all DOFs for the parameter screening.

Acceleration (LLTB)						
	DOF1	**LSA1**	**DOF2**	**LSA2**	**DOF3**	**LSA3**
Baseline	19.0		13.7		9.8	
Block & bed plate side mass	17.5	0.079	13.3	0.029	10.2	-0.041
Block & bed plate side stiffness	17.5	0.079	13.3	0.029	10.2	-0.041
Crank shaft general stiffness	9.0	0.526	14.1	-0.029	12.8	-0.306
Crank shaft shank stiffness	13.1	0.311	13.1	0.044	12.0	-0.224
Cylinder head mass	17.7	0.068	13.4	0.022	10.0	-0.020
Cylinder head stiffness	17.2	0.095	14.3	-0.044	9.2	0.061
Main bearing clearance	18.3	0.037	12.7	0.073	9.9	-0.010
RHM mass	19.0	0.000	13.9	-0.015	9.6	0.020
RHM stiffness	18.9	0.005	13.9	-0.015	9.6	0.020
STD	15.2		12.2		10.3	
Cylinder no. 1 retardation	14.1	0.072	12.0	0.016	10.7	-0.039
Cylinder no. 1-4 retardation	13.9	0.086	10.3	0.156	10.9	-0.058
Cylinder no. 4 retardation	14.4	0.053	10.2	0.164	12.8	-0.243
Combustion duration						
Long	15.3	-0.007	10.8	0.115	10.9	-0.058
Short	15.3	-0.007	12.3	-0.008	9.7	0.058

D Right hand mount design study PAPR data

In Tables D.1, D.2, D.3, D.4, D.5, D.6, D.7, D.8, D.9 and D.10 the velocity and the acceleration PAPR data for the RHM design study, combined with each DOFs sensitivity metric, for the RHM, the LHM, the RUTB, the RLTB and the LLTB, respectively, are presented.

The comparison of the absolute PAPR values for the different mounting points has lead to the selection of the RHM in the vertical direction as the most relevant and important to study

D.1 RHM

Table D.1: All calculated PAPR data for the velocity in the RHM with corresponding SA metrics for all DOFs for the RHM design study.

Velocity (RHM)						
	DOF1	**LSA1**	**DOF2**	**LSA2**	**DOF3**	**LSA3**
Baseline	17.6		15.1		23.8	
Left & right block support	11.2	0.364	11.6	0.232	11.4	0.521
Right block support	13.5	0.233	14.0	0.073	10.3	0.567
Block top support	21.1	-0.199	13.0	0.139	23.0	0.034
Bed plate support	8.6	0.511	12.7	0.159	11.7	0.508
Cylinder head support	10.7	0.392	14.2	0.060	11.7	0.508
Suspension point support	16.7	0.051	12.2	0.192	8.5	0.643
Left & right block hinged support	18.8	-0.068	16.0	-0.060	24.8	-0.042
Block top hinged support	16.9	0.040	15.2	-0.007	24.5	-0.029
Bed plate hinged support	13.4	0.239	13.6	0.099	16.3	0.315

Table D.2: All calculated PAPR data for the acceleration in the RHM with corresponding SA metrics for all DOFs for the RHM design study.

Acceleration (RHM)						
	DOF1	**LSA1**	**DOF2**	**LSA2**	**DOF3**	**LSA3**
Baseline	30.8		18.6		43.8	
Left & right block support	17.7	0.425	13.7	0.263	32.0	0.269
Right block support	16.6	0.461	17.9	0.038	30.9	0.295
Block top support	28.2	0.084	18.1	0.027	44.2	-0.009
Bed plate support	15.6	0.494	14.7	0.210	28.4	0.352
Cylinder head support	17.4	0.435	21.4	-0.151	31.7	0.276
Suspension point support	19.0	0.383	15.5	0.167	29.3	0.331
Left & right block hinged support	34.2	-0.110	21.3	-0.145	42.7	0.025
Block top hinged support	34.0	-0.104	17.7	0.048	44.0	-0.005
Bed plate hinged support	26.9	0.127	16.7	0.102	29.4	0.329

D.2 LHM

Table D.3: All calculated PAPR data for the velocity in the LHM with corresponding SA metrics for all DOFs for the RHM design study.

Velocity (LHM)						
	DOF1	**LSA1**	**DOF2**	**LSA2**	**DOF3**	**LSA3**
Baseline	13.1		9.4		10.9	
Left & right block support	12.4	0.053	9.1	0.032	10.9	0.000
Right block support	12.4	0.053	9.3	0.011	10.7	0.018
Block top support	13.0	0.008	9.5	-0.011	10.8	0.009
Bed plate support	12.1	0.076	9.3	0.011	10.7	0.018
Cylinder head support	12.8	0.023	9.2	0.021	10.9	0.000
Suspension point support	12.7	0.031	9.3	0.011	10.9	0.000
Left & right block hinged support	13.5	-0.031	9.4	0.000	10.7	0.018
Block top hinged support	13.0	0.008	9.4	0.000	10.7	0.018
Bed plate hinged support	13.0	0.008	9.4	0.000	10.6	0.028

Table D.4: All calculated PAPR data for the acceleration in the LHM with corresponding SA metrics for all DOFs for the RHM design study.

Acceleration (LHM)						
	DOF1	**LSA1**	**DOF2**	**LSA2**	**DOF3**	**LSA3**
Baseline	20.8		11.1		19.5	
Left & right block support	19.5	0.063	12.2	-0.099	18.9	0.031
Right block support	19.3	0.072	14.7	-0.324	18.8	0.036
Block top support	20.6	0.010	11.8	-0.063	19.7	-0.010
Bed plate support	18.9	0.091	12.3	-0.108	18.4	0.056
Cylinder head support	20.3	0.024	11.6	-0.045	19.2	0.015
Suspension point support	20.1	0.034	11.1	0.000	19.2	0.015
Left & right block hinged support	20.1	0.034	13.5	-0.216	19.2	0.015
Block top hinged support	20.7	0.005	11.1	0.000	19.3	0.010
Bed plate hinged support	19.5	0.063	11.0	0.009	19.1	0.021

D.3 RUTB

Table D.5: All calculated PAPR data for the velocity in the RUTB with corresponding SA metrics for all DOFs for the RHM design study.

Velocity (RUTB)						
	DOF1	**LSA1**	**DOF2**	**LSA2**	**DOF3**	**LSA3**
Baseline	11.6		9.1		8.5	
Left & right block support	13.5	-0.164	7.2	0.209	9.1	-0.071
Right block support	12.6	-0.086	6.9	0.242	9.7	-0.141
Block top support	11.8	-0.017	8.8	0.033	8.0	0.059
Bed plate support	13.0	-0.121	6.9	0.242	9.0	-0.059
Cylinder head support	12.7	-0.095	8.2	0.099	8.4	0.012
Suspension point support	12.9	-0.112	8.2	0.099	8.0	0.059
Left & right block hinged support	11.7	-0.009	9.0	0.011	9.7	-0.141
Block top hinged support	11.5	0.009	9.1	0.000	8.6	-0.012
Bed plate hinged support	11.2	0.034	8.2	0.099	10.8	-0.271

Table D.6: All calculated PAPR data for the acceleration in the RUTB with corresponding SA metrics for all DOFs for the RHM design study.

Acceleration (RUTB)						
	DOF1	**LSA1**	**DOF2**	**LSA2**	**DOF3**	**LSA3**
Baseline	17.7		11.4		12.1	
Left & right block support	15.4	0.130	14.2	-0.246	9.5	0.215
Right block support	16.6	0.062	14.8	-0.298	11.1	0.083
Block top support	17.3	0.023	13.5	-0.184	12.7	-0.050
Bed plate support	15.8	0.107	13.7	-0.202	11.0	0.091
Cylinder head support	16.9	0.045	13.4	-0.175	10.8	0.107
Suspension point support	16.0	0.096	19.2	-0.684	14.2	-0.174
Left & right block hinged support	17.6	0.006	10.3	0.096	11.4	0.058
Block top hinged support	17.7	0.000	12.2	-0.070	11.5	0.050
Bed plate hinged support	17.9	-0.011	18.5	-0.623	18.0	-0.488

D.4 RLTB

Table D.7: All calculated PAPR data for the velocity in the RLTB with corresponding SA metrics for all DOFs for the RHM design study.

Velocity (RLTB)						
	DOF1	**LSA1**	**DOF2**	**LSA2**	**DOF3**	**LSA3**
Baseline	8.4		16.8		15.0	
Left & right block support	7.8	0.071	16.6	0.012	14.6	0.027
Right block support	8.2	0.024	16.3	0.030	15.3	-0.020
Block top support	8.2	0.024	16.9	-0.006	15.2	-0.013
Bed plate support	7.8	0.071	16.3	0.030	14.6	0.027
Cylinder head support	8.0	0.048	16.6	0.012	15.0	0.000
Suspension point support	8.2	0.024	16.7	0.006	14.7	0.020
Left & right block hinged support	8.3	0.012	16.6	0.012	15.8	-0.053
Block top hinged support	8.3	0.012	16.9	-0.006	15.1	-0.007
Bed plate hinged support	9.7	-0.155	16.6	0.012	15.2	-0.013

Table D.8: All calculated PAPR data for the acceleration in the RLTB with corresponding SA metrics for all DOFs for the RHM design study.

Acceleration (RLTB)						
	DOF1	**LSA1**	**DOF2**	**LSA2**	**DOF3**	**LSA3**
Baseline	16.7		24.3		37.0	
Left & right block support	15.8	0.054	24.5	-0.008	36.2	0.022
Right block support	17.1	-0.024	23.9	0.016	37.8	-0.022
Block top support	16.7	0.000	24.4	-0.004	37.3	-0.008
Bed plate support	15.0	0.102	24.1	0.008	36.4	0.016
Cylinder head support	16.4	0.018	24.0	0.012	36.6	0.011
Suspension point support	16.7	0.000	24.2	0.004	36.5	0.014
Left & right block hinged support	17.0	-0.018	24.6	-0.012	39.0	-0.054
Block top hinged support	16.6	0.006	24.3	0.000	37.0	0.000
Bed plate hinged support	19.3	-0.156	24.2	0.004	37.0	0.000

D.5 LLTB

Table D.9: All calculated PAPR data for the velocity in the LLTB with corresponding SA metrics for all DOFs for the RHM design study.

Velocity (LLTB)						
	DOF1	**LSA1**	**DOF2**	**LSA2**	**DOF3**	**LSA3**
Baseline	15.3		8.0		6.6	
Left & right block support	14.7	0.039	8.0	0.000	6.7	-0.015
Right block support	14.9	0.026	8.1	-0.013	6.8	-0.030
Block top support	15.1	0.013	8.0	0.000	6.8	-0.030
Bed plate support	14.8	0.033	7.9	0.013	6.7	-0.015
Cylinder head support	15.3	0.000	8.1	-0.013	6.5	0.015
Suspension point support	15.3	0.000	8.1	-0.013	6.5	0.015
Left & right block hinged support	14.0	0.085	8.1	-0.013	6.5	0.015
Block top hinged support	15.3	0.000	8.1	-0.013	6.5	0.015
Bed plate hinged support	15.1	0.013	8.1	-0.013	6.5	0.015

Table D.10: All calculated PAPR data for the acceleration in the LLTB with corresponding SA metrics for all DOFs for the RHM design study.

Acceleration (LLTB)						
	DOF1	**LSA1**	**DOF2**	**LSA2**	**DOF3**	**LSA3**
Baseline	19.0		13.7		9.8	
Left & right block support	18.6	0.021	13.9	-0.015	10.1	-0.031
Right block support	18.3	0.037	14.1	-0.029	10.2	-0.041
Block top support	18.9	0.005	13.9	-0.015	9.9	-0.010
Bed plate support	18.6	0.021	13.7	0.000	10.0	-0.020
Cylinder head support	18.9	0.005	13.8	-0.007	9.9	-0.010
Suspension point support	18.9	0.005	13.8	-0.007	9.8	0.000
Left & right block hinged support	16.9	0.111	14.1	-0.029	9.9	-0.010
Block top hinged support	18.9	0.005	13.7	0.000	9.7	0.010
Bed plate hinged support	18.3	0.037	13.7	0.000	10.1	-0.031